Vol2 No2
July 2022
e-ISSN: 2682-9177

AJMed TECH

ASIAN JOURNAL OF MEDICAL TECHNOLOGY

https://doi.org/10.32896/ajmedtech.v2n2

https://ajmedtech.com

eISSN 2682-9177

Editorial Team

ASIAN JOURNAL OF MEDICAL TECHNOLOGY

Contents

Volume 2 **Number 2** **July 2022**

balt solutions
for AVM treatment

squid
EVOH co-polymer

sonic
detachable tip microcatheter

balt
inspiring innovation

Join us for Hands-On
AVM Workshops. Register your interest with
carlteh@medcinpharma.com / hiba@medcinpharma.com

MEDCIN PHARMA SDN BHD (587084 - D)

Imported and distributed by :
Medcin Pharma Sdn Bhd (587084-D)
H-G-3A, Blok H, Sekitar 26 Enterprise,
Persiaran Hulu Selangor, Seksyen 26,
40400 Shah Alam, Selangor Darul Ehsan
Tel: +60 (03) 5192 3966
Fax: +60 (03) 5191 9539
http://www.medcinpharma.com

ESTABLISHMENT OF RQT BEAM QUALITY (100 TO 150 kV) FOR COMPUTED TOMOGRAPHY APPLICATIONS

N.N.M. Rais[1, 2], N.M. Noor[1, 3*], A. Hashim[4], D.A. Bradley[5, 6], N.D. Osman[7], I. Ismail[8] and H.A. Hassan[9]

[1]Medical Physics Laboratory, Department of Radiology, Faculty of Medicine and Health Sciences, Universiti Putra Malaysia, 43400, Serdang, Selangor, Malaysia.

[2]Department of Diagnostic Imaging and Radiotherapy, Kulliyyah of Allied Health Sciences, International Islamic University Malaysia, 25200, Kuantan, Pahang, Malaysia.

[3]Medical Physics Unit, Teaching Hospital Universiti Putra Malaysia, Universiti Putra Malaysia, 43400, Serdang, Selangor, Malaysia

[4]Medical Physics Laboratory, Malaysian Nuclear Agency, 43000, Kajang, Selangor Malaysia.

[5]Department of Physics, University of Surrey, GU2 7XH, Guildford, Surrey, United Kingdom.

[6]Centre for Applied Physics and Radiation Technologies, Sunway University, 47500, Bandar Sunway, Selangor, Malaysia.

[7]Advanced Medical and Dental Institute, Universiti Sains Malaysia, 13200, Kepala Batas, Pulau Pinang, Malaysia.

[8]Department of Medicine, Faculty of Medicine and Health Sciences, Universiti Putra Malaysia, 43400, Serdang, Selangor, Malaysia.

[9]Department of Radiology, Faculty of Medicine and Health Sciences, Universiti Putra Malaysia, 43400, Serdang, Selangor, Malaysia.

[*]Corresponding Author's Email: noramaliza@upm.edu.my

Article History: Received March 10, 2022; Revised May 12, 2022; Accepted May 27, 2022

ABSTRACT: In Malaysia, the radiation beam qualities for calibration of dosimeters in computed tomography (RQT series) were established at the Secondary Standard Dosimetry Laboratory (SSDL) of the Malaysian Nuclear

Agency by using a constant potential industrial X-ray machine and a 0.6 cc PTW UNIDOS ionization chamber calibrated at the International Atomic Energy Agency (IAEA). Through the experimental method of additional filtration determination, the results demonstrated that all measured first half-value layer (HVL) filtrations (mm Al) for each RQT 8 (100 kV), RQT 9 (120 kV) and RQT 10 (150 kV) comply with tolerance limits of ± 3% as recommended by the IEC-61676. For RQT 8, a repeated experiment to determine accurate additional filtration has to be done with different added filtration RQT (mm Cu) thickness as the value initially goes beyond the 3% difference. Compared to prior radiation quality series RQT determinations, the added filtration for RQT 8 changed from 0.1 mm Cu in 2019 to 0.2 mm Cu in 2020. When compared against values established over the previous three years, all three RQTs for 2020 exhibit differences in measured first HVL filtrations (mm Al), albeit remaining within the 3% difference standard recommended in the TRS 457 standard of the IAEA. This change arises from x-ray tube ageing, anode roughening and inherent filtration alteration, leading to a perceived need for RQT trial and error re-evaluation to reduce the percentage decrement. Yearly monitoring of the beams should be performed to determine possible radiation quality changes, taking corrective action where necessary to remain within the prescribed tolerance limit. The standard radiation qualities should be maintained, allowing calibration accuracy to confirm dosimeter readings.

KEYWORDS: *RQT Radiation Quality; Malaysian Nuclear Agency; Dosimetry Calibration.*

1.0 INTRODUCTION

There is an undeniably increasing usage worldwide for medical imaging examinations, particularly in general radiography, fluoroscopy, and computed tomography (CT). In regards to the continuous emergence of the latest and advanced medical diagnostic equipment, the higher amount of radiation that the patients, radiographers, and medical workers are expected to receive directly or indirectly from these imaging procedures is becoming a primary concern. Even though the probability of radiation-induced malignancy caused by ionizing imaging tools is relatively low, the rise in per capita dose due to the growth in the number of individuals receiving these medical imaging examinations contributes to the need for controlled patient dosimetry [1]. In light of the significance of radiation dosimetry to the patients and the medical workers, the concept of dose

optimization in accords to ALARA (as low as reasonably achievable) without jeopardizing the image quality has to be established together with regulatory control. Numerous codes of practice, written handbooks and technical reports have been issued globally to regulate radiology procedures and beam qualities by contributing to the establishment of Diagnostic Reference Levels (DRLs) such as the International Commission on Radiation Units and Measurements [2], International Electrotechnical Commission [3] and International Atomic Energy Agency [4].

The principle of DRLs was presented by the International Commission on Radiological Protection [5] and has been generally acknowledged as a practical means for dose optimization in medical imaging. DRLs should be applied as a method of investigation for patient exposure to identify unusually high dose levels. If DRLs are consistently exceeded, a local review normally ensues. As such, a review of patient dosimetry in a clinical setting is essential in terms of successful DRLs implementation. Direct dose measurement of radiation patients receive during medical imaging examinations is the initial step toward successful DRLs implementation. The measurements could be accomplished by means of radiation dose measured via dosimeters calibrated against a standard measuring system. It is essential that the used dosimeters were properly calibrated and accommodated in reference to IEC 61267 [3] and TRS 457 [4] as reference beam qualities for the calibration of instruments in medical imaging and radiology. Such calibration for the instrument is important as incident radiation is a major factor that can distort their energy responses [6].

The primary concept in establishing radiation quality for dosimetry calibration is to recreate a condition in which whilst it must be of a comparable environment to those encountered in routine use of the dosimetry instrument. In addition, it must be able to facilitate reproducible methodology between different dosimetry laboratories. According to Green et al. [7], the established form of calibration traceability regarding standard radiation dosimetry begins with the calibration of dosimeters by a Primary Standard Dosimetry Laboratory (PSDL). The same instrument and calibration setup are then used at the Secondary Standard Dosimetry Laboratory (SSDL) to reproduce the beam quality that closely matches the PSDL, to transfer the calibration from the Secondary Standard Dosimeter to a Tertiary Standard

Dosimeter. This Tertiary Standard Dosimeter is then used to define the radiation exposure for diagnostic instruments and dosimetry tools in which calibrated irradiations are to be tested in the clinical setting. Therefore, it is essential to establish radiation quality that is within the dynamic range used in real clinical practice. The quality of these instruments to measure X-ray outputs are critical for the upcoming valuation and patient doses regulator delivered by the hospital equipment. This article will discuss one of the established methods for precise calibration of dosimetry instruments in terms of investigating RQT radiation quality at SSDL in the Malaysian Nuclear Agency.

An X-ray beam spectra distribution for dosimeter calibrations had been discussed in detail by Green et al. [7-8]. The X-ray beam's utmost comprehensive description is characterized by its spectral distribution. To establish specific radiation quality, the portrayal of these beam qualities in the form of X-ray tube voltage (kV) and the first half-value layer (HVL) is normally applied since the spectrometry of X-rays necessitates a substantial amount of in-field competency, and it also takes longer duration to be accomplished. A concession amongst the equally inconsistent needs of evading extreme methodology to establish a radiation quality and warranting any uncertainty in the description of the radiation quality amongst many diagnostic imaging centres has led to the documentation of the standardized International Code of Practice TRS 457 [4].

Uncertainty in radiation quality in diagnostic imaging centres has led to the standardized International Code of Practice [4], the radiation qualities generated by X-ray tubes displaying inconsistencies in terms of tube age (with anode roughness and inherent filtration influences) and constructional differences (e.g., anode angle). This work concerns year-to-year changes in radiation quality. Malaysian Nuclear Agency has established a Secondary Standard Dosimetry Laboratory (SSDL), the national standard typically being referenced against the International Atomic Energy Agency (IAEA) primary standard, not least for calibration of dosimeters.

Table 1, including the listing of typical applications, concerns radiation qualities implemented for diagnostic imaging dosimeter calibrations. In line with TRS 457 [4], the beam qualities are established with reference to International Electrotechnical Commission IEC 61267 [3] recommendations. For measurement of the first HVL, the added filtration technique has been used, as documented by the International Commission on Radiation Units and Measurements [2]. This requires

the use of a narrow-beam geometry to mitigate against in-scattering. The field incident on the ionization chamber (IC) must expose the entire IC for accurate measurement. At the Malaysian Nuclear Agency, a 2 cm diameter circular collimator is used, providing a field of 7 cm diameter at 100 cm source image distance (SID).

RQT radiation qualities that simulate the un-attenuated beam applied in computed tomography (CT) have been sought herein, determining the copper (Cu) filtration that may need to be added to the previously established RQR beam qualities. Annual assessment of first HVL filtration allows comparison against prior values, with corrections ensuring that differences do not exceed 3% [4]. Herein, a periodic establishment for RQT radiation quality at the Malaysian Nuclear Agency is detailed.

Table 1: Radiation qualities for calibration of diagnostic dosimeters [4]

Radiation quality	Radiation origin	Material of additional filter	Application
RQR	Radiation beam emerging from X-ray assembly	No phantom	General radiography, fluoroscopy and dental applications (measured free in air)
RQA	Radiation beam with an added filter	Aluminium	Measurements behind the patient (on the image intensifier)
RQT	Radiation beam with an added filter	Copper	CT applications (measured free in air)
RQR-M	Radiation beam emerging from X-ray assembly	No phantom	Mammography applications (measured free in air)
RQA-M	Radiation beam with an added filter	Aluminium	Mammography studies

2.0 METHODOLOGY

RQT beam quality measurements have been established at the Malaysian Nuclear Agency using a secondary standard 0.6 cc PTW UNIDOS ionization chamber instrument calibrated at the IAEA with Cu and Al filters of different thicknesses being slotted in front of a Constant Potential Philips Industrial X-Ray Model MG165 (Table 2). At the chamber's position, a field size of 7 cm diameter at 100 cm source image distance (SID) was established, obtained by slotting in a 2 cm diameter collimator in front of the added filters, ensuring a low scatter

good geometry situation (Figure 1). The beam current and irradiation time were fixed at 5 mA for 50 s, respectively, applied for each radiation quality: RQT 8 (100 kV), RQT 9 (120 kV) and RQT 10 (150 kV). All the measurements for established radiation qualities had been performed in an air environment free of other perturbing materials, such as dosimetry phantoms, water, or other scattering materials. Temperature, pressure and relative humidity recordings were monitored and kept constant throughout the measurements.

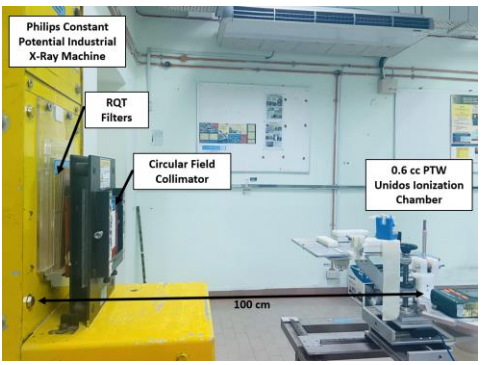

(a)

(b)

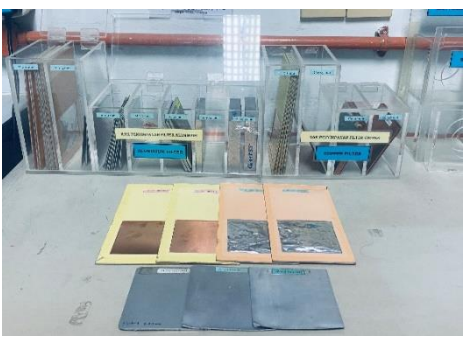

(c)

Figure 1: (a) Philips Constant Potential Industrial X-ray machine with filters aligned with 0.6cc PTW Unidos ionization chamber, (b) control panel at SSDL, Malaysian Nuclear Agency, (c) close-up of Al and Cu added filters

Table 2: RQT series for the period 2016 to 2019, within 3% agreement with IAEA values at the Malaysian Nuclear Agency

Radiation quality	X-ray tube voltage (kV)	Added filtration RQR (mm Al)	Added filtration RQT (mm Cu)	Total filtration RQR (mm Al) + RQT (mm Cu)	First HVL filtration (mm Al)	
					IAEA	Measured
RQT 8	100	3.7	0.1	3.7 + 0.1	6.9	6.7
RQT 9	120	4.0	0.2	4.0 + 0.2	8.4	8.4
RQT 10	150	4.8	0.2	4.8 + 0.2	10.1	10.1

Initial exposures were made in the absence of HVL filtration; the dose was recorded. In subsequent exposures, Al filters of different thicknesses were slotted in front of the collimator. Maintaining the initial technical factors, exposures were then made using different Al filter thicknesses. A linear graph of normalized dose against Al thickness was anticipated, allowing the first HVL filtration to be acquired via interpolation. HVL filtration must remain within 3% of that of prior years, with reference to the period 2016 to 2019. The RQT beam qualities were measured every year for the period 2016 to 2019, and the results for those four years were consistent. As referred to in Table 2, the measured results were in good agreement with the standard (IAEA) for both RQT 9 and 10, while the percentage of difference for RQT 8 was 2.89%, albeit within the acceptable range of 3%. For values exceeding 3%, trial and error use has been made of added Cu filtration, measuring the air kerma as before, with and without first HVL Al filtration.

3.0 RESULTS AND DISCUSSIONS

3.1 RQT 8 Additional Filtration Determination

As shown in Table 3, the determination of filtration for RQT 8 (100 kV) was initiated by slotting in RQR added filters, with 3.7 mm Al and RQT added filtration of 0.1 mm Cu, according to the previously established RQR beam quality maintained over the period 2016-2019 (Table 2). In the absence of HVL filters, the average dose is 15.1 mGy, as shown in Table 3. Subsequent HVL filters are then added within the recorded range of mm Al thickness for the first HVL filtration. A linear graph of

normalized average doses against subsequent Al thicknesses is obtained (Figure 2). Concerning Figure 2, it is evident that the nominal first HVL filtration for RQT 8 is 6.2 mm Al, compared to the IAEA tabulated value of 6.9 mm Al. Beam hardening is evident, amounting to a decrease of 10.1 % in HVL value when referenced against the IAEA recommended value of 6.9 mm Al, exceeding the tolerance of 3%. This is suggested to be due to ageing of the x-ray tube, a manifestation of anode roughening and build-up of inherent filtration [4]. As such, RQT added filter (Cu) has to be added by trial and error, seeking to reduce the percentage decrement.

Table 3: Determination of additional filtration for characterization of radiation quality RQT 8

Radiation quality	X-ray tube voltage (kV)	Added filtration RQR (mm Al) + RQT (mm Cu)	HVL filter (mm Al)	Average dose (mGy)	First HVL filtration (mm Al)		Diff (%)
					IAEA	Measured	
RQT 8	100	3.7 + 0.1	0	15.1	6.9	6.2	10.1
			5.0	8.3			
			6.0	7.5			
			7.0	6.8			
			8.0	6.1			

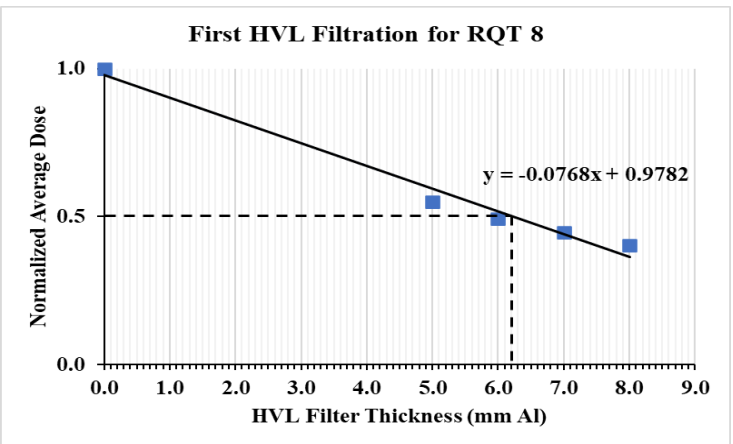

Figure 2: Measured first HVL filtration (mm Al) for RQT 8

Repeat determination of additional filtration for RQT 8 is shown in Table 4. RQR added filters of 3.7 mm Al thickness were slotted in front of the X-ray tube. However, instead of the previous use of 0.1 mm Cu, use has now been made of an increment of 0.2 mm Cu. With these new added filters, measurements were then made using the same technical factors as before, with values recorded in column 5, Table 4. As before, a linear graph of normalized average dose versus Al thickness has been obtained (Figure 3), allowing the first HVL filtration to be acquired, as represented by the dotted line in Figure 3. The new HVL filtration is found to be 6.9 mm Al (column 7, Table 4), being in accord with the recommended value of the IAEA [4]. The re-establishment of RQT 8 radiation quality at the Malaysian Nuclear Agency for the year 2020 has thus been obtained.

Table 4: Repeat determination of additional filtration for characterization of radiation quality RQT 8

Radiation quality	X-ray tube voltage (kV)	Added filtration RQR (mm Al) + RQT (mm Cu)	HVL filter (mm Al)	Average dose (mGy)	First HVL filtration (mm Al)		Diff (%)
					IAEA	Measured	
RQT 8	100	3.7 + 0.2	0	10.9	6.9	6.9	0
			5.0	6.6			
			6.0	5.9			
			7.0	5.5			
			8.0	4.9			

3.2 RQT 9 Additional Filtration Determination

A similar determination has been made for RQT 9 (120 kV), as referred to in Table 5. At 120 kV, using a constant 5 mA for 50 s, Table 5 shows close accord to have been realized within 3% of the IAEA nominal first HVL filtration of 8.4 mm Al. The linear graph of normalized average dose against Al thickness is shown in Figure 4. The measured first HVL filtration of 8.3 mm Al is shown in column 7, Table 5, amounting to a beam-hardening decrease in HVL of 1.2 %. Less than 3% change is deemed acceptable, with no repeat measurements necessary.

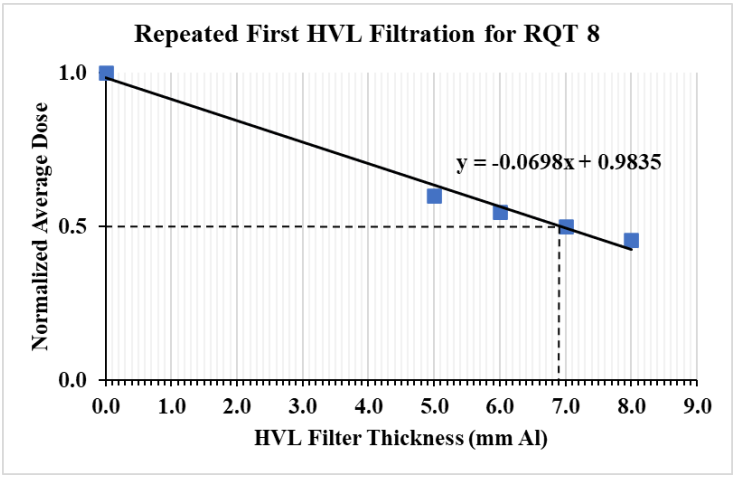

Figure 3: Repeated measurement of first HVL filtration (mm Al) for RQT 8

Table 5: Determination of additional filtration for characterization of radiation quality RQT 9

Radiation quality	X-ray tube voltage (kV)	Added filtration RQR (mm Al) + RQT (mm Cu)	HVL filter (mm Al)	Average dose (mGy)	First HVL filtration (mm Al)		Diff (%)
					IAEA	Measured	
RQT 9	120	4.0 + 0.2	0	17.1	8.4	8.3	1.2
			7.0	9.3			
			8.0	8.6			
			9.0	7.9			
			10.0	7.3			

3.3 RQT 10 Additional Filtration Determination

Finally, in Table 6, the record is made of RQR 4.8 mm Al added filters and RQT 0.2 mm Cu added filters, initially slotted in front of the x-ray tube to determine RQT 10 (150 kV). The reference IAEA first HVL filtration for RQT 10 is 10.1 mm Al [4]. In subsequent exposure, an HVL filter of total Al thickness of 9.0 mm was slotted in front of the collimator, the average of five readings being recorded, a step repeated for incremental Al thicknesses of total value 10-, 11- and 12 mm. Figure 5 shows a linear graph of normalized average dose against Al thickness. The calculated first HVL filtration of RQT 10 is 9.9 mm Al (column 7, Table 5). This amounts to a decrease of 2.0 % in HVL when

compared to the reference value of 10.1 mm Al. As for the previous section, this change with respect to the prior value established at the Malaysian Nuclear Agency and the IAEA reference value is within the 3% tolerance. Re-establishing RQT 10 at Malaysian Nuclear Agency for 2020 is deemed successful with no change of added filtration RQR (mm Al) and RQT (mm Cu) thickness required.

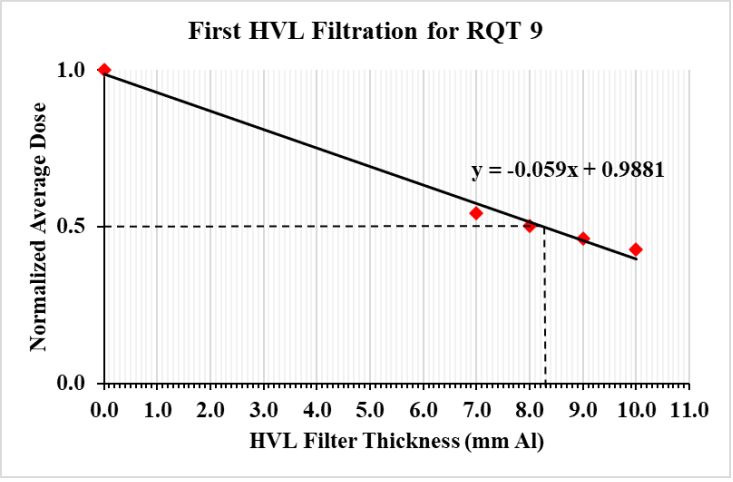

Figure 4: Measured first HVL filtration (mm Al) for RQT 9

Table 6: Determination of additional filtration for characterization of radiation quality RQT 10

Radiation quality	X-ray tube voltage (kV)	Added filtration RQR (mm Al) + RQT (mm Cu)	HVL filter (mm Al)	Average dose (mGy)	First HVL filtration (mm Al)		Diff (%)
					IAEA	Measured	
RQT 10	150	4.8 + 0.2	0	27.4	10.1	9.9	2.0
			9.0	14.0			
			10.0	13.2			
			11.0	12.4			
			12.0	11.6			

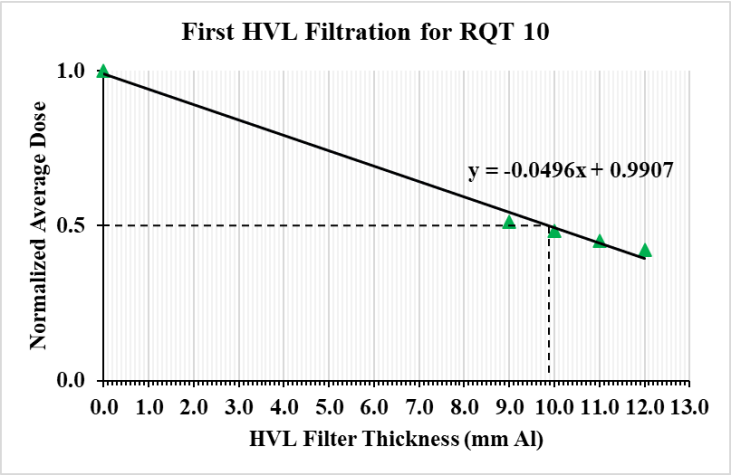

Figure 5: Measured first HVL filtration (mm Al) for RQT 10

3.4 Re-establishment of RQT Radiation Quality

Table 7 shows the final RQR (mm Al) total added filtration and RQT (in mm Cu), measured for the first HVL filtration. Compared to the RQT radiation quality series established from 2016 to 2019 at the Malaysian Nuclear Agency (Table 2), the added filtration for RQT 8 changed from 0.1 mm Cu in 2019 to 0.2 mm Cu in 2020. When compared against previous years, all three RQTs measured in 2020 differ from the baseline HVL filtrations (mm Al), nevertheless remaining within 3% of the recommended TRS 457 values [4]. In other words, the results demonstrated that all three measured RQTs' first HVL filtrations (mm Al) complied with the tolerance limits of ± 3% as recommended by the IEC-61267 [3]. The compliance of the results indirectly substantiated that SSDL in Malaysian Nuclear Agency is maintaining its standard of practice and quality control of periodic radiation quality establishment, particularly in sustaining the ageing of the x-ray tube, anode roughening and inherent filtration. Unsurprisingly, given the increasingly greater influence of the photoelectric effect as spectral distribution shifts towards lower energies, the change was greatest for the RQT 8 series.

Table 7: Re-establishment of radiation quality series RQT at Malaysian Nuclear Agency for the year 2020

Radiation quality	X-ray tube voltage (kV)	Added filtration RQR (mm Al)	Added filtration RQT (mm Cu)	Total filtration RQR (mm Al) + RQT (mm Cu)	First HVL filtration (mm Al)	
					IAEA	Measured
RQT 8	100	3.7	0.2	3.7 + 0.2	6.9	6.9
RQT 9	120	4.0	0.2	4.0 + 0.2	8.4	8.3
RQT 10	150	4.8	0.2	4.8 + 0.2	10.1	9.9

4.0 CONCLUSION

Periodic RQT radiation quality measurements have been performed at the Malaysian Nuclear Agency Secondary Standard Dosimetry Laboratory to calibrate dosimeters in CT applications. Use has been made of a Philips constant potential industrial X-ray machine supported by a 0.6 cc PTW UNIDOS ionization chamber calibrated at the IAEA. The results show that all three RQT first HVL filtrations (mm Al) comply with the ± 3% tolerance limit recommended in IEC 61267. For RQT 8, to provide for conformity, a repeat experiment was conducted to determine the additional filtration required to account for beam hardening of the x-ray tube. This new value may be due to the ageing of the x-ray tube in terms of anode roughening and inherent filtration. As such, an RQT added filter (Cu) must be added, obtained through trial and error, taking into account the percentage difference. Yearly monitoring on the first HVL filtration of the beams should be performed to test for changes with respect to prior values, seeking to maintain the accuracy of standard radiation qualities for calibrating diagnostic dosimeters, not least for CT applications.

5.0 ACKNOWLEDGEMENTS

The staff of the Secondary Standard Dosimetry Laboratory and Medical Physics Laboratory at Malaysian Nuclear Agency, also Department of Radiology, Faculty of Medicine and Health Sciences, Universiti Putra Malaysia are acknowledged for assisting in this study. Universiti Putra Malaysia funding was provided under an FRGS/1/2018/STG02/UPM/02/7 grant from the Ministry of Higher

Education, Malaysia.

6.0 REFERENCES

[1] V. S. Panyam, S. Rakshit, S. D. Dhole et al., "Methodology adopted to establish diagnostic X-ray beam qualities", *Applied Radiation and Isotopes*, vol. 150, pp. 164-167, 2019.

[2] *International Commission on Radiation Units and Measurements, Physical Aspects of Irradiation, National Bureau of Standards Handbook*, ICRU, Bethesda, Maryland, 1964.

[3] *International Electrotechnical Commission, Medical Diagnostic X-Ray Equipment - Radiation Conditions for Use in the Determination of Characteristics*, IEC 61267, IEC, Geneva, 2005.

[4] *International Atomic Energy Agency, Dosimetry in Diagnostic Radiology: An International Code of Practice,* TRS 457, IAEA, Vienna, Austria, 2007.

[5] *Radiological Protection and Safety in Medicine. A Report of the International Commission on Radiological Protection*, ICRP 26, ICRP, Ottawa, Ontario, 1997.

[6] S. M. Tajudin, Y. Namito, T. Sanami, and H. Hirayama. "Photon field of ~100–200 keV for environmental dosemeter calibration", *Radiation Protection Dosimetry,* vol. 188, pp. 486-492, 2020.

[7] S. Green, J. E. Palethorpe, D. Peach, and D. A. Bradley. "Performance assessment of patient dosimetry services and X-ray quality assurance instruments used in diagnostic radiology", *Applied Radiation and Isotopes*, vol. 50, pp. 137-152, 1999.

[8] S. Green, J. E. Palethorpe, D. Peach, and D. A. Bradley. "Development of a calibration facility for test instrumentation in diagnostic radiology", *Radiation Protection Dosimetry,* vol. 67, pp. 41-46, 1996.

SMART MULTIPARAMETER INFANT APNOEA MONITOR

S.C. Nwaneri[1*], B.N. Ezenwa[2], A.A. Osuntoki[3], V.C. Ezeaka[2], D.W. Gatchell[4] and F.T. Ogunsola[5]

[1]Department of Biomedical Engineering, Faculty of Engineering, University of Lagos, 132, Akoka Yaba, Lagos, Nigeria.

[2]Department of Paediatrics, College of Medicine, 132, Akoka Yaba, Lagos, Nigeria.

[3]Department of Biochemistry, College of Medicine, 132, Akoka Yaba, Lagos, Nigeria.

[4]Department of Biomedical Engineering, Northwestern University, 60208, Evanston, Illinois, United States of America.

[5]Department of Medical Microbiology and Parasitology, College of Medicine, 132, Akoka Yaba, Lagos, Nigeria.

[*]Corresponding Author's Email: snwaneri@unilag.edu.ng

Article History: Received March 14, 2022; Revised April 11, 2022; Accepted May 29, 2022

ABSTRACT: Apnoea is a common disorder in preterm infants who may also suffer from neonatal hypertension. Conventional apnoea monitors used in neonatal intensive care units (NICUs) do not include features for measuring neonatal blood pressure and real-time remote monitoring. Smart devices to monitor this problem in resource-poor environments are expensive and sparsely available. This paper presents the development of a smart multiparameter infant apnoea monitor in a resource-poor setting. The circuit was designed and simulated in Proteus software. The signals were processed using Arduino mega microcontrollers. The microcontroller concurrently communicates apnoea events to the GSM modem and alarm which notify the doctor and caregivers by SMS alert and audible alarm, respectively. Preliminary testing on stable infants at the NICU of Lagos University Teaching Hospital showed promising results. The device can effectively be used to monitor apnoea in infants as well as transmit the results to the doctor in a remote location by SMS. It can also be used to monitor other parameters like

oxygen saturation, respiratory rate, heart rate and blood pressure. The documented experiences will provide useful insights for smart infant apnoea to monitor development in resource-poor environments.

KEYWORDS: *Infant Apnoea, Preterm, Internet of Things, Neonatal Hypertension, Pulse Oximetry Sensor.*

1.0 INTRODUCTION

Apnoea is a respiratory disorder characterized by momentary pauses in breathing or momentary or sustained reductions in breath amplitude in an individual, leading to significant arterial hypoxemia and hypercapnia [1]. In infants, this condition is commonly associated with prematurity. It is defined as the cessation of breathing for a minimum of 20 seconds or lesser periods in the presence of bradycardia, cyanosis or other evidence of oxygen desaturation [2]. The incidence of apnoea is high among critically ill babies globally [3]. In particular, it is a leading cause of perinatal and neonatal mortality in resource-poor countries [4][5][6]. The disorder has been linked to several undesirable health conditions such as repeated hypoxemia, asphyxia [1], poor neurodevelopmental outcome and even death. Preterm infants are not only prone to apnoea. Still, they are also predisposed to other respiratory diseases due to the poor development of mechanisms of respiratory control, especially in their first year of life [7][8]. Therefore, frequent monitoring of their breathing patterns, especially during sleep, is necessary.

Neonatal hypertension is common in preterm infants, which necessitates frequent blood pressure (BP) monitoring in infants admitted to neonatal intensive care units (NICU) [9][10]. Regular non-invasive BP measurements are invaluable in babies, especially in the first early days of life [11][12][13]. In addition, it is necessary to monitor their oxygen saturation and heart rate frequently. Oxygen saturation is detected using pulse oximetry and arterial blood gases (ABG) [14]. Several innovative approaches have been previously used in the design of apnoea monitors. The gold standard for apnoea diagnosis is the use of polysomnography (PSG) [15][16]. PSG involves continuous, simultaneous multi-channel measurements of eight different physiological signals, including oronasal flow, oxygen saturation and heart rate, electroencephalography (EEG, brain waves), electro-oculography (EOG, eye movements), chin electromyography (muscle

activity), electrocardiography (ECG), respiratory effort and airflow. Unfortunately, such testing is expensive, burdensome, time-consuming, and typically carried out for very limited periods in a foreign environment. It is complicated and expensive to use in resource-poor settings [17].

The project aims to develop a smart multiparameter infant apnoea monitor that can detect the incidence of apnoea in infants and monitor other important parameters such as respiratory rate, oxygen saturation, heart rate and blood pressure. The device was conceived due to the shortage of functional apnoea monitors in the NICU of a tertiary hospital in Southwest Nigeria. The main significance of this study is the potential reduction in infant mortality with successful deployment and availability of the device. Also, it can enhance the performance of physicians who would be enabled to monitor the health condition of critically ill patients remotely.

2.0 LITERATURE REVIEW

Research on apnoea monitor design and development has received significant interest [18]. A home sleep test (HST) was proposed by [19] as a well-validated alternative to PSG. HST has fewer sensors than PSG and is more compact, less expensive, and less cumbersome to use with little or no support from a technologist. Oliver and Flores-Mangas [20] built an automatic sleep apnoea detection and a monitoring system comprising physiological sensors wirelessly connected via Bluetooth. While in [21], the authors developed a sleep apnoea detection and monitoring device, which only requires two data channels: tracheal breathing sounds and pulse oximetry (SaO_2 signal). Considering the high risk of sleep apnoea, some medical device manufacturers have adopted a pulse oximeter which measures the oxygen saturation level in the blood, which is believed to decrease by 4% once there is the cessation of airflow in the lungs for at least 10 seconds [21]. Also, authors in [22] developed an IoT-based sleep apnoea monitoring system that helps users monitor different indexes of sleep and notify the physician through a mobile platform when apnoea occurs.

Furthermore, in [23], the authors proposed using multimodality sensors to observe rest by utilizing a non-intrusive and low-cost sleep-wake detection system that detects early symptoms of sleep disorders. Also, in [24], a sleep apnoea detection system was designed and developed. While in [25], wearable e-textile sensors utilized an IoT

method to collect real-time data on sleeping behaviours and respiratory rate. In another study, [26] developed a smart healthcare monitoring system based on the Internet of Things (IoT) to enable remote monitoring of patients on the internet. The device consists of pulse oximetry and temperature sensors for detecting apnoea and monitoring temperature.

In recent years, there has been a significant increase in the demand for health monitoring devices both in industry and research. The benefits of these wearable health monitoring technologies are enormous since they could enable the detection of early signs of health deterioration; notify health care providers in critical situations; enhance the sense of connectedness with loved ones by sharing real-time raw or interpreted physiological data; find correlations between lifestyle and health and transform health care by providing physicians with real-time data amongst others [27]. Garde *et al.* [28] used a phone oximeter, a portable device integrating pulse oximetry with a smartphone, to detect obstructive sleep apnoea. However, in order to make these wearable devices more practical, they need to be non-intrusive, comfortable to wear, consume power efficiently, have a user-friendly interface by preserving privacy, have a minimal failure rate and have highly accurate alarm triggers especially if used for diagnostic purposes. The available breathing monitoring systems are both expensive and invasive [20]. Tewel [29] developed an apnoea monitor for infant monitoring using a microelectromechanical (MEMS) accelerometer. The device focused primarily on monitoring the breathing movements of the infant's abdomen without considering other vital parameters.

Conventional infant apnoea monitors have limited features and cannot inform the doctor of apnoeic episodes remotely. The use of mobile phones and the internet is prevalent in Nigeria. According to the Nigerian Communications Commission (NCC), Nigeria has a high internet penetration rate of 144, 949, 194 million [30]. There is a need to develop a smart infant apnoea monitor that also includes the monitoring of arterial blood pressure of preterm infants. Blood pressure (BP) measurement is an important vital sign to monitor in infants admitted to NICU to assess adequate circulation and tissue perfusion in the newborn, which is often not measured in conventional infant apnoea monitors.

Furthermore, doctors need real-time remote monitoring of the patient by doctors, which will greatly benefit providing urgent response during an emergency. The developed device can simultaneously monitor apnoeic episodes, pulse rates, and blood pressures in infants and is suitable for home and hospital use to send instant messages to the doctor in a remote location using the Internet of Things (IoT). To the best of our knowledge, there is no commercially available smart infant apnoea monitor which combines respiratory rate, heart rate and blood pressure monitoring in infants with IoT capability with considerations for unstable electricity supply.

3.0 MATERIALS AND METHODS

3.1 Device design and requirements

The study was approved by the College of Medicine, University of Lagos Health Research and Ethics Committee (CMUL/HREC/03/18/342). Informed consent was obtained from the parents of the participants. Device requirements are summarized based on the American Society for Testing and Materials (ASTM) standard requirements in Table 1. Identified risks for the device and mitigation measures are shown in Table 2.

Table 1: Device requirements

S/N	Characteristics	Requirement
1	Medical	User-specified SPO2, heart rate, respiratory rate and blood pressure
2	Economic	Low cost
3	Mechanical	Portable DC Powered
4	User-interface	Visual display of settings and status
5	Repeatability	Indicators within 10% of correct reading

Table 2: Risk mitigation strategies

Risk	Mitigation Measures
Inadequate Alarms	A red LED indicator is used as a visible alarm to indicate apnoea An audible alarm is activated once apnoea occurs
Electrical Shock	The device is powered by low power DC batteries and adequately insulated to prevent exposure to electric shock
Inaccurate Detection	Signal amplification and filtering were incorporated into

	the design to enhance detection accuracy. The sensor measurement interface was designed to improve contact with the subject.
Tissue Reactivity	The device was built with biocompatible materials with no tissue reaction

The translation of ideas into preliminary rough sketches is the first step. Afterwards, computer-aided design (CAD) was developed. The benefits of CAD in product development are well known. Hence, a 3D CAD design for the device was produced, as shown in Figure 1.

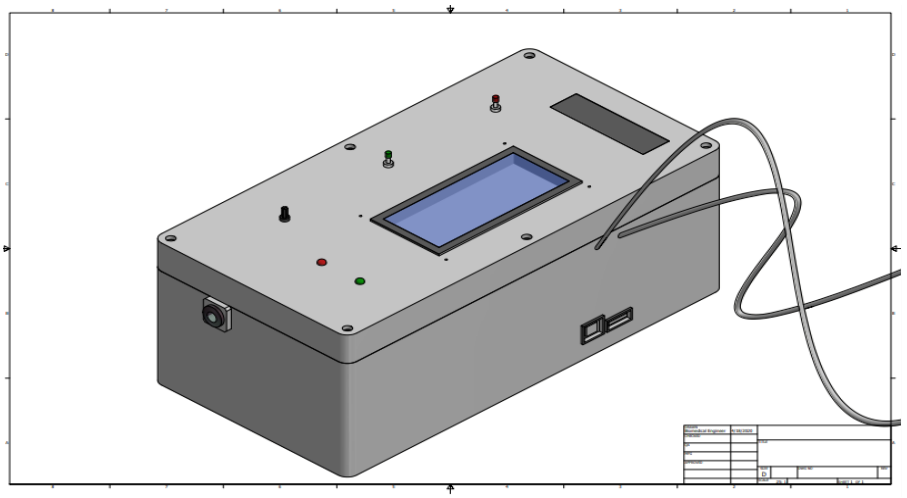

Figure 1: 3D CAD Design of Infant Apnoea Monitor

3.2 Device description

The device consists of the following sections; power supply, sensors, signal amplification and filtering, microcontrollers, graphical display, alarm and GSM module. The block diagram of the device shown in Figure 2 describes the entire system.

The device was powered by rechargeable Lithium-ion cells. The circuit included three sensors: an accelerometer, pulse oximetry and heart rate biosensor, and a blood pressure sensor. The accelerometer (ADXL335) was used for measuring respiratory rate (RR) as well as

apnoea detection, pulse oximetry and heart rate biosensor (MAX30100) was used for oxygen saturation and heart rate measurement, and the blood pressure sensor was for blood pressure measurement. Signal conditioning was achieved with signal filtering and instrumentation amplifier circuit. The circuit was constructed with an Arduino Mega 2560 microcontroller board which operates as a master and interfaced with four slave ATMEGA 328 microcontrollers. The master coordinates the communication and drives the display. The first slave was dedicated to the accelerometer sensor. The second slave was connected to the pulse oximetry and heart rate biosensor module, and the third slave, was connected to the pressure sensor, while the fourth slave microcontroller ensured an uninterrupted connection with the online server. The output includes a graphical liquid crystal display (GLCD), an audible alarm and the GSM module. The GSM module includes a registered subscriber identity module (SIM) card configured to send instant messages to a mobile phone once apnoea occurs through a Thingspeak IoT platform.

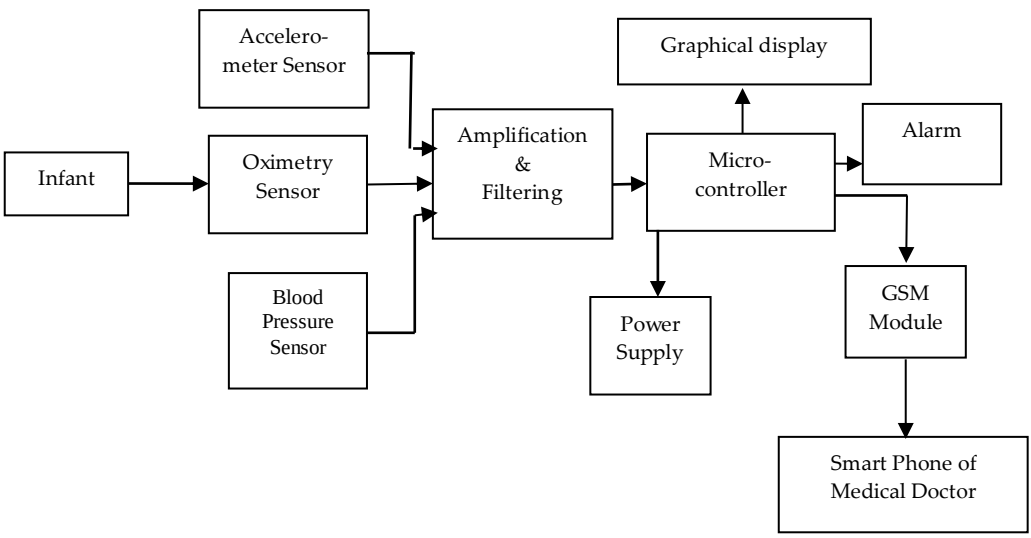

Figure 2: Block Diagram of the Smart Multiparameter Apnoea Monitor

3.3 Theoretical Framework

Apnoea detection is based on the ability of the accelerometer to measure the rate of change of the velocity of people and objects by sensing either static or dynamic forces of acceleration. It is generally

used to measure acceleration on one, two, or three axes [31]. In healthcare systems, accelerometers are combined with light, and flexible, electronic components that do not interfere with normal human motion and activities [32]. The design of an accelerometer is based on Newton's law of mass acceleration and Hooke's law of spring action, which implies that the mass undergoing acceleration exerts a force opposed to the restraining effect of spring [33]. For spring of mass M, damping coefficient D, spring coefficient K, external force F, and acceleration a, the movement of the spring is modelled by a second-order differential equation (1):

$$M\frac{d^2x}{dt^2} + D\frac{dx}{dt} + kx(t) = Ma(t) \quad (1)$$

The device was developed using a microelectromechanical sensor (MEMS) accelerometer, which operates based on the principle of capacitive sensing. In this study, the principle is applied to the conversion of body displacement of the MEMS accelerometer caused by breathing movements of the user to a change in capacitance which can be expressed as:

$$\Delta C = C_1 - C_2 \quad (2)$$

But,

$$C_1 = \varepsilon\frac{A}{d - x} \quad (3)$$

$$C_2 = \varepsilon\frac{A}{d + x} \quad (4)$$

Where, C_1 and C_2 = capacitances of the plates of the two capacitors.

$A =$ Area of the plates

$d =$ proof mass displacement

When apnoea occurs, there is no acceleration. Hence, $C_1 = C_2$. Therefore, $\Delta C = 0$. However, the differential capacitance increases when breathing is restored as $\Delta C > 0$. Signals from the accelerometer are sampled at a frequency of 3.4 Hz based on the sampling theorem. Given that a continuous signal does not have a frequency component higher than W Hz, the sampling frequency, fs of the signal is calculated as:

$$f_s \geq 2W \quad (5)$$

Conversely, the integrated pulse oximetry and heart rate biosensor

module monitor oxygen levels and pulse rate. The principle of pulse oximetry is based on the absorption of different wavelengths of light. Red and infrared light is absorbed by oxygenated and deoxygenated haemoglobin differently. The sensor determines oxygen saturation in the blood using red and infrared light frequencies. The ratio between red and infra-red light is defined in equations (6) and (7) [34]:

$$R = \frac{\mathrm{AC_{RMS\ RED}}/\mathrm{DC_{RED}}}{\mathrm{AC_{RMS\ IR}}/\mathrm{DC_{IR}}} \tag{6}$$

$$\mathrm{R} = \frac{\log(\mathrm{I_{AC}}) + \lambda_1}{\log(\mathrm{I_{AC}}) + \lambda_2} \tag{7}$$

Where $\mathrm{I_{AC}} =$ Light intensity where only AC is present

$\lambda_1 =$ Wavelength of red light

$\lambda_2 =$ Wavelength of Infrared light

$\mathrm{R} =$ Ratio of ratios

The oxygen saturation is therefore calculated as shown in (8):

$$\mathrm{SpO_2} = 110 - 25 \times \mathrm{R} \tag{8}$$

Blood pressure monitoring was implemented based on the oscillometric method, one of the most widely used blood pressure measurements in automatic cuff devices [35]. The blood pressure is measured non-invasively by occluding the brachial artery using external neonatal cuffs [36]. Mean arterial pressure (MAP) is attained [37]. While systolic and diastolic pressure are empirically estimated in accordance with the fixed ratio algorithm [38]. Enhancement of signal quality and noise removal was achieved by filtering. The fourth-order active bandpass filter was designed using multiple feedback (MFB) topology in accordance with methods proposed by [39]. Further processing of signals was achieved using the moving average digital signal processing (DSP) method. This technique takes an average of prescribed points in the signal to yield each point in the output signal [40]:

$$\mathrm{y[i]} = \frac{1}{\mathrm{M}} \sum_{\mathrm{j=0}}^{\mathrm{M-1}} \mathrm{x[i+j]} \tag{9}$$

Where $\mathrm{x}[i+j] =$ input signal

$\mathrm{y}[i] =$ output signal

$M = \text{Number of points}$

Thus, the moving average filter smoothened the signal and decreased random noise. The mode selector chooses the parameters to be tested to test the device. The first mode includes respiratory rate, oxygen saturation and heart rate. At the same time, blood pressure is the only parameter included in the second mode. Apnoea condition is determined by placing the accelerometer around the abdomen to detect abdominal movement during breathing. The infant must lie in a supine position. When apnoea occurs, the regular abdominal movement ceases for at least 20 seconds. The accelerometer is unable to detect any abdominal movements. Hence, this information is transmitted to a buzzer alarm. The alarm is activated to notify nurses and caregivers that apnoea has occurred.

Similarly, the physician receives an instant SMS notification on their mobile phone. Instant SMS notification was achieved with a Sim800L GSM module configured to send data to the Thingspeak IoT platform. This configuration enables the doctor to access and store the results from a remote location. The device is reset after turning off the alarm before using it again.

The blood pressure circuit includes a pressure sensor that detects the pressure and transmits the results to the microcontroller, which sends it to the visual display. In testing the blood pressure, the neonatal cuff with a limb circumference of 6 to 11 cm is attached to the neonate's arm and inflated. The pressure sensor detects the differential pressure between atmospheric and blood pressure. The systolic and diastolic blood pressure is displayed on the digital display.

4.0 RESULTS AND DISCUSSION

The proof of concept (POC) was subjected to pilot testing in the NICU of Lagos University Teaching Hospital. The preliminary tests were performed on only stable infants for safety reasons, and there were no reported side effects. Fig. 3 shows the POC with the values of the heart rate, SpO_2, and respiratory rate of a sample test indicated respectively by the visual display.

Figure 3: The POC Smart Infant Apnoea Monitor

Regular breathing in humans is associated with abdominal movements. The 3D printed casing of the accelerometer is placed on the subject's abdomen to detect regular abdominal movements to detect apnoea. The cessation of the abdominal movement for at least 20 seconds is an indication that apnoea has occurred. The accelerometer detects this. The alarm turns on, and the device also sends an SMS to a phone configured Arduino program. The mean SPO_2, respiratory rates and heart rate results are shown in Table 3.

Table 3: Results of SPO_2, RR and HR

	SpO_2	**Respiratory Rate (RR)**	**Heart Rate**
Mean	95.17	30.08	81.33
Standard Deviation	1.53	3.34	14.13

Table 4: Results of Blood Pressure Measurements

	Systolic	**Diastolic**
Patient A	96	62
Patient B	82	63
Patient C	85	64

The mean ± standard deviation observed for SpO_2 (%), RR (cycles per minute), and HR (Beats per minute) for the POC were (95.17±1.53; 30.08±3.34 and 81.33±14.13). The blood pressure readings from three infants are shown in Table 5. The results were comparable to that of a standard device. Some innovative features have been incorporated into the device to improve its usefulness. Regular monitoring of apnoea occurrence in a neonate is essential as nursing documentation has been considered inadequate [41]. This will help the physician to independently assess the progress made in treatment even while not physically present. However, the design also includes an audible alarm which notifies medical personnel or caregivers physically present to enable them to provide quick intervention. Biological signals are not only weak but also non-deterministic and thus generally produce varying output values. We demonstrated that signal quality could be enhanced by digital signal processing and an efficient filtering system. Figure. 4 shows the output analogue voltage produced by the MEMS accelerometer when the accelerometer is placed on a subject. As observed, the signal is characterized by noise. However, the application of moving average filtering to the raw signalled improves signal quality and noise reduction, as observed in Figure 5.

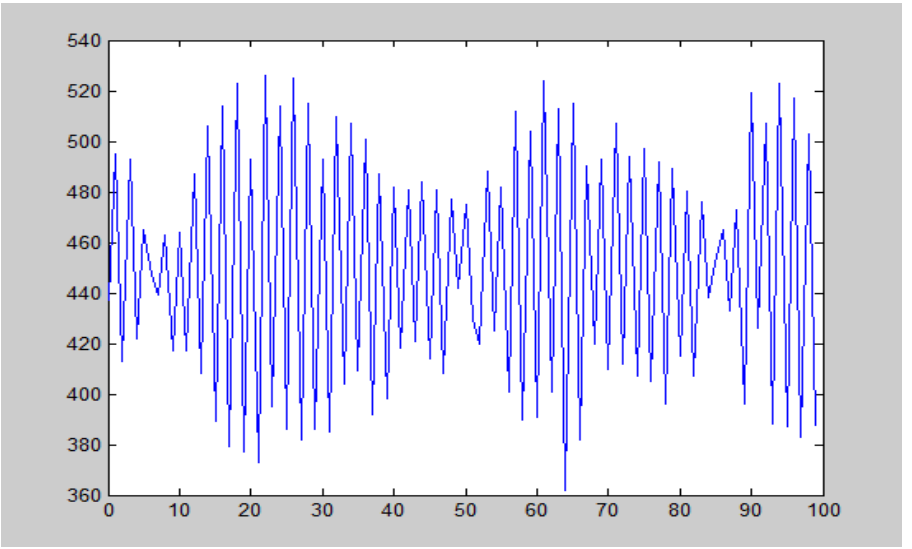

Figure 4: Raw Data from Y-axis of stationary sensor

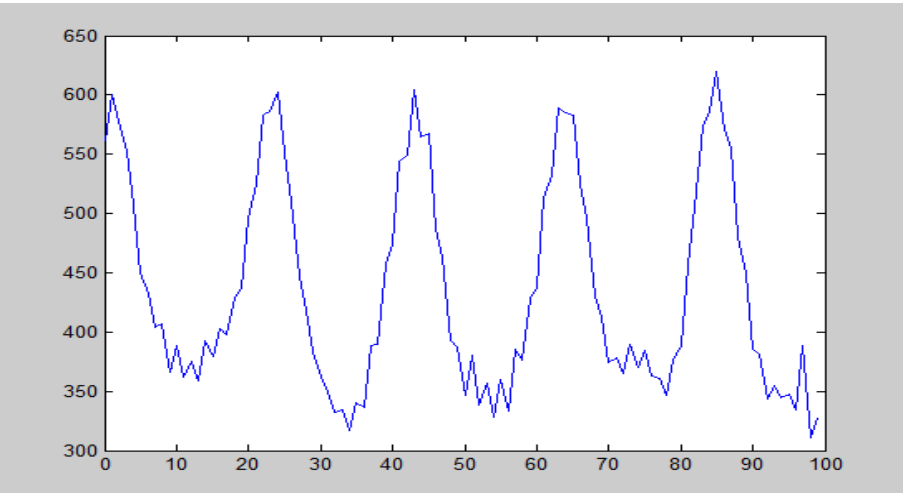

Figure 5: Moving average filtered data from Stationary object z-axis

Furthermore, 3D printed sensor casing was shown to provide a smooth measurand-sensor interface, enhancing the device's effectiveness. To the best of our knowledge, this study is one of the few to develop a smart multiparameter infant apnoea monitor for neonates in a resource-poor environment. The benefits of this device include its ability to send instant SMS to notify the physician of apnoeic episodes. It can also be used at home to monitor infants' apnoea and basic vital signs even after being discharged from the hospital. When there is a need to return to the hospital based on the regular alerts received by the physician, the parents can be called to return the baby to the clinic for further observations and treatments.

The development of smart infant apnoea monitors has enormous prospects and huge market potential, given the prevalence of the disease in resource-poor settings. We also observed significant improvements in signal quality using high gain instrumentation amplifiers for signal amplification. This agrees with previous studies that described the benefits of instrumentation amplifiers for biomedical applications [42]. The use of a biocompatible, non-toxic sensor casing is an important factor to consider in developing medical devices, particularly in infants, for obvious safety reasons. Product development processes for such medical devices require effective project and supply chain management strategies. Proactive measures to mitigate the supply chain gaps in component sourcing will greatly

impact product development. The main limitation is the occasional inability to detect precise breathing movements. Also, the alarm is beeping when apnoea is detected and needs to be reset.

5.0 CONCLUSIONS

In this paper, we discussed the development of a smart multiparameter infant apnoea monitor in a resource-poor setting and an evaluation of its performance. The study presented documented problems experienced in the device development, especially those peculiar to resource-poor settings and their possible solutions. The developed device showed good prospects when tested. Further investigations will be done on the utility of the device.

6.0 ACKNOWLEDGEMENTS

Research reported in this publication was supported by the Fogarty International Center of the National Institutes of Health under Award Number D43TW010134. The content is solely the authors' responsibility and does not necessarily represent the official views of the National Institutes of Health. Co-funding partners include Fogarty International Center (FIC), NIH Common Fund, Office of Strategic Coordination, Office of the Director (OD/OSC/CF/NIH), Office of AIDS Research, Office of the Director (OAR/NIH), Office of Research on Women's Health, Office of the Director (ORWH/NIH), National Institute on Minority Health and Health Disparities (NIMHD/NIH), and National Institute of Neurological Disorders and Stroke (NINDS/NIH).

7.0 REFERENCES

[1] J.A. Dempsey, S.C. Veasey, B.J. Morgan, C.P. O'Donnell, "Pathophysiology of Sleep Apnea", *Physiological Reviews*, 90, pp. 47 – 112, 2010.

[2] S. Picone, R. Aufieri, P. Paolillo, "Apnea of prematurity: challenges and solutions", *Research and Reports in Neonatology*, vol. 4, pp. 101 - 109, 2014.

[3] J.M. Rennie, N.R. Robertson, Apnoiec attacks, In: J.M. Rennie, G. Kendall (Eds.), *A manual of neonatal intensive care, fourth ed.*, Oxford:Arnold Publishers, pp. 216 – 222, 2002.

[4] C.L. Huddy, A. Johnson, P.L. Hope, "Educational and behavioral problems in babies of 32–35 weeks gestation", *Archives of Disease in Childhood (Fetal Neonatal Ed.*), vol. 85, 23F-8, 2001.

[5] A. Tamene, G. Abeje, and Z. Addis, "Survival and associated factors of mortality of preterm neonates admitted to Felege Hiwot specialized hospital, Bahir Dar, Ethiopia", *Sage Open Medicine*, 2020, https://doi.org/10.1177/2050312120953646.

[6] T.A. Ogunlesi, O.B. Ogunfowora, "Pattern and determinants of newborn apnea in an under-resourced Nigerian setting", *The Nigerian Journal of Clinical Practice*, vol. 15, pp. 159 – 164, 2012.

[7] A. Janvier, M. Khairy, A. Kokkotis, C. Cormier, D. Messmer, K.J. Barrington, "Apnoea is associated with neurodevelopmental impairment in very low birth weight infants", *Journal of Perinatology*, vol. 24, pp. 763 – 768, 2004.

[8] N.L. Maitre, R.A. Ballard, J.H. Ellenberg, S.D. Davis, J.M. Greenberg, A. Hamvas, G.S. Pryhuber, "Respiratory consequences of prematurity: evolution of a diagnosis and development of a comprehensive approach", *Journal of Perinatolology*, vol. 35, no. 5, pp. 313 – 321, 2015.

[9] R.H. Steinhorn, "Neonatal Pulmonary Hypertension", *Pediatric Critical Care Medicine*, vol. 11, pp. 79 – 84, 2010.

[10] A. Nickavar, F. Assadi, "Managing Hypertension in the Newborn Infants". *International Journal of Preventive Medicine*, vol. 5, no. 1, pp. S39 - S43, 2014.

[11] S. Cunningham, A.G. Symon, R.A. Elton, "Intra-arterial blood pressure reference ranges, death and morbidity in VLBW infants in the first 7 days of life", *Early Human Development*, vol. 56, pp. 151 – 156, 1999.

[12] M. Di Biase, A. Casani, L. Orfeo, "Invasive arterial blood pressure in the neonatal intensive care: a valuable tool to manage very ill preterm and term neonates", *Italian Journal of Pediatrics*, vol. 41(suppl 1), 2015 doi: 10.1186/1824-7288-41-S1-A9.

[13] N. Kumar, G. Akangire, B. Sullivan, et al. "Continuous vital sign analysis for predicting and preventing neonatal diseases in the twenty-first century: big data to the forefront". *Pediatric Research*, vol. 87, pp. 210–220, 2020, https://doi.org/10.1038/s41390-019-0527-0.

[14] S. Seifi, A. Khatony, G. Moradi, A. Abdi, F. Najafi, "Accuracy of pulse oximetry in detection of oxygen saturation in patients admitted to the intensive care unit of heart surgery: comparison of finger, toe, forehead and earlobe probes", *BMC Nursing*, vol. 17, no. 15, 2018, https://doi.org/10.1186/s12912-018-0283-1.

[15] A. Abrishami, A. Khajehdehi, F. Chung, "A systematic review of screening questionnaires for obstructive sleep apnea", *Canadian Journal of Anesthesia*, vol. 57, no. 5, pp. 423 – 438, 2010.

[16] S.M. Caples, W. M. Anderson, K. Calero, M. Howell, S.D. Hashmi. Use of polysomnography and home sleep apnea tests for the longitudinal management of obstructive sleep apnea in adults: an American Academy of Sleep Medicine clinical guidance statement. *Journal of Clinical Sleep Medicine*, vol. 17, no. 6, pp. 1287-1293, 2021, doi: 10.5664/jcsm.9240.

[17] A. Roebuck, V. Monasterio, E. Gederi, M. Osipov, J. Behar, A. Malhotra, T. Penzel, G.D. Clifford, "A review of signals used in sleep analysis", *Physiological Measurement*, vol. 35, pp. R1 – 57, 2014.

[18] Y. Fang, Z. Jiang, H. Wang, "A Novel Sleep Respiratory Rate Detection Method for Obstructive Sleep Apnea Based on Characteristic Moment Waveform", *Journal of Healthcare Engineering*, 2018, https://doi.org/10.1155/2018/1902176.

[19] M. Kapoor, G. Greenough, "Home Sleep Tests for Obstructive Sleep Apnea (OSA)", *Journal of the American Board of Family Medicine*, vol. 28, no. 4, pp. 504 – 509, 2015.

[20] N. Oliver, F. Flores-Mangas, "HealthGear: Automatic Sleep Apnea Detection and Monitoring with a Mobile Phone", *Journal of Communications*, vol. 2, no. 2, pp. 1 – 9, 2007.

[21] A. Yadollahi, E. Giannouli, Z. Moussavi, "Sleep apnea monitoring and diagnosis based on pulse oximetry and tracheal sound signals", *Medical and Biological Engineering and Computing*, vol. 48, pp. 1087–1097, 2010.

[22] A. R. Dhruba, K.N. Alam, S. Khan, S. Bourouis, M.M. Khan, "Development of an IoT Based Sleep Apnoea Monitoring System for Health Applications", vol. 2021, Article 7152576 16 pages, 2021, https://doi.org/10.1155/2021/7152576

[23] S.R. Sawale, V.S. Gulhane, "Multimodality Sensor System for Sleep -

Quality Monitoring", *International Journal of Computer Science and Mobile Computing*, vol. 3, pp. 564 – 571, 2014.

[24] M. Gaiduk, L. Weber, A.S. Alarcon, R. Seepold, N.M. Madrid, S. Orcioni, and M. Conti, "Design of a sleep apnoea detection system for a home environment", *Procedia Computer Science*, vol. 192, pp. 3225 – 3234, 2021.

[25] G. Cay and K. Mankodiya, "SleepSmart: smart mattress integrated with e-textiles and IoT functions for sleep apnea management," in *2020 IEEE International Conference on Pervasive Computing and Communications Workshops (PerCom Workshops)*, pp. 1-2, Austin, USA, 2020.

[26] B.K. Bhoomika, K.N. Muralidhara, "Secured Smart Health Monitoring System Based on IoT", *International Journal on Recent Innovation Trends in Computing and Communication*, vol. 3, no. 7, pp. 4958 -4961, 2015.

[27] B.S. Ranjitha, "Non-invasive sleep apnea detection and monitoring system", *International Research Journal of Engineering and Technology*, vol. 3, pp. 1196 – 1202, 2016.

[28] A. Garde, P. Dehkordi, W. Karlen, D. Wensley, J.M. Ansermino, and G.A. Dumont, "Development of a Screening Tool for Sleep Disordered Breathing in Children Using the Phone Oximeter", PLUS ONE, 2014, https://doi.org/10.1371/journal.pone.0112959.

[29] N. Tewel, "Application of MEMS accelerometer for baby apnea monitoring under home conditions", *Acta Bio-Optica et Informatica Medica*, vol. 16, pp. 389 – 393, 2010.

[30] Nigerian Communication Commission, "Active Internet Subscriptions by Technology January 2021 – December 2021", https://www.ncc.gov.ng/statistics-reports/industry-overview#view-graphs-tables-5, 2022 (accessed 3 February 2022).

[31] R.F. Tinder, *Relativistic Flight Mechanics and Space Travel: A Primer for Students, Engineers and Scientists*. California: Morgan & Claypool Publishers, 2007.

[32] G. Ciuti, L. Ricotti, A. Menciassi, P. Dario, "MEMS Sensor Technologies for Human Centred Applications in Healthcare, Physical Activities, Safety and Environmental Sensing: A Review on Research Activities in Italy", *Sensors*, vol. 15, pp. 6441 – 6468, 2015.

[33] A.V. Bakshi U.A. Bakshi, *Instrumentation*. Pune: Technical Communications, 2009.

[34] J. G. Webster, Ed., *Design of Pulse Oximeters*, 1st ed. New Jersey:Taylor & Francis, 1997.

[35] A. Chandrasekhar, C. Kim, M. Naji, K. Natarajan, J. Hahn, and R. Mukkamala, "Smartphone-based blood pressure monitoring via the oscillometric finger pressing method", *Science Translation Medicine*, 2018, https://doi.org/10.1126/scitranslmed.aap8674.

[36] C.F. Babbs, "Oscillometric measurement of systolic and diastolic blood pressures validated in a physiologic mathematical model", *Biomedical Engineering Online*, vol. 11, 2012, https://doi.org/10.1186/1475-925X-11-56.

[37] S. Lopez, Blood Pressure Monitor Fundamentals and Designs, Free Scale Semiconductor Eichenwald, EC Committee on Fetus and Newborn, "Apnoea of prematurity". *Pediatrics*, vol. 137, 1, e20153757, 2012, https://doi.org/10.1542/peds.2015-3757.

[38] A. Chandrasekhar, M. Yavarimanesh, J.O. Hah, S.H. Sung, C.H. Chen, H.M. Cheng, R. Mukkamala. "Formulas to Explain Popular Oscillometric Blood Pressure Estimation Algorithms". *Frontiers in Physiology*, vol. 10, 1415, 2019, https://doi.org/10.3389/fphys.2019.01415

[39] A H. Abd, "Design and simulation of 4th order active bandpass filter using multiple feedback and Sallen-key topologies", *Journal of Babylon University of Engineering Sciences*, vol. 22, 2014, ceca8bad4ee05e7c (iasj.net)

[40] S.W. Smith, *The Scientist and Engineer's Guide to Digital Signal Processing*, California:Technical Publications, 1999.

[41] S.B. Amin and E. Burnell, "Monitoring Apnea of Prematurity: Validity of Nursing Documentation and Bedside Cardiorespiratory Monitor", *American Journal of Perinatology*, vol. 30, pp. 643 – 648, 2013.

[42] G. Sathiyabama,G.Vinudevi, R. Abhilashini, P.Indhupriya, "A Survey on Instrumentation Amplifiers used for Biomedical Application", *International Journal of Advanced Research in Electrical and Electronics Instrumentation Engineering*, vol. 4, 2015.

TRACKABLE-SPECKLE DETECTION USING A DUAL-PATH CONVOLUTIONAL NEURAL NETWORK FOR NODES SELECTION IN SPECKLE TRACKING ECHOCARDIOGRAPHY

M. Shiri[1,*], H. Behnam[1], H. Yeganegi[2], Z.A. Sani[3] and N. Nematollahi[1]

[1]Department of Biomedical Engineering, School of Electrical Engineering, Iran University of Science and Technology, 1684613114, Narmak, Tehran, Iran.

[2]Graduate School of Systemic Neurosciences, Ludwig Maximilians University, Grosshaderner Street 2, D-82152, Planegg, Munich, Germany.

[3]Rajaie Cardiovascular Medical & Research Center, Tehran University of Medical Sciences, 1416634793 , Keshavarz, Tehran, Iran.

[*]Corresponding Author's Email: milad70shiri@gmail.com

Article History: Received March 30, 2022; Revised April 19, 2022; Accepted May 25, 2022

ABSTRACT: Speckle tracking echocardiography (STE) is widely used to quantify regional motion and deformation of heart tissues. Before tracking, a segmentation step is first carried out, and only a set of nodes in the segmented model are tracked. However, a random selection of the nodes even after tissue segmentation could lead to an inaccurate estimation. In this paper, a convolutional neural network (CNN)-based method is presented to detect trackable speckle spots that have important properties of the texture for speckle tracking. The proposed CNN was trained and validated on 29500 ultrasound manually labelled image patches extracted from the echocardiography of 65 people. Using the proposed network, in silico experiments for automatic node selection were conducted to investigate the applicability of the proposed method in speckle tracking. The results were statistically highly significant (P<.001) and demonstrated that the proposed method has the least tracking error among various existing methods.

KEYWORDS: *Speckle Detection, Convolutional Neural Network, Ultrasound Imaging, Echocardiography*

1.0 INTRODUCTION

Ultrasound imaging is a promising modality for medical diagnosis, mostly because it is non-invasive, cheap and easy to use [1-3]. Echocardiography, in particular, is an ultrasound-based tool for cardiac imaging which is vastly used for identifying heart defects [4]. In addition to visual assessment of the heart, many computer-aided and fully automatic techniques have been proposed for qualitative and quantitative cardiac function evaluations [5-7]. Tracking the myocardium and calculating its elasticity provides us with a common method of quantifying the mechanical activity of the heart [8]. Two-dimensional (2D) speckle tracking is commonly used for tissue tracking based on ultrasound B-mode images. [9,10].

Speckles are the bright points seen in an echocardiogram, which are the results of diffuse scattering [10]. Since speckles are caused by interference of backscattered signals from extremely small neighbouring elements in the tissue, the speckle pattern is strictly correlated with the microstructure of the underlying tissue [11]. As a result, the topological pattern of closely-connected speckles is usually similar over consecutive frames and can be used for tracking [12]. However, speckles are not always suitable for tracking and could lead to misestimating displacements in speckle tracking. Hence, speckle detection algorithms are not useful for spotting trackable speckle patterns.

Speckle tracking methods essentially use mentioned property of speckle pattern to estimate the displacement of desired points between two or more frames. Occasionally, speckle tracking is carried out for each point of the entire image or at least of the segmented model [9,12]. But more likely, a segmentation is first carried out, and only a selection of nodes is tracked. Either way, nodes should be selected wisely in a suitable way for tracking purposes; otherwise, it could lead to miscalculation of displacement, even for a node selected randomly or manually from the segmented region[13]. The tracking nodes are usually selected manually and occasionally automatically based on textural features. Manually selecting nodes depends on the observer's precision and is often difficult to proceed. Therefore, automatic node selection methods are preferred for their accuracy and speed compared to observer's judgment. As explained in [14] and [11], speckle characterization and detection methods are useful for selecting important and informative regions of the image and, therefore, node selection.

The earliest approaches for image-based speckle characterization were mostly based on the extraction of the first-order features. Mean, variance, skewness, kurtosis and energy are some of these texture statistics that can be calculated from the first-order histogram of the gray level image. Speckle discrimination properties of statistics were evaluated by Prager et al. [15] using a combination of simulations and the homodyned-k distribution. Marti et al. [16] presented a fully automatic speckle detection method by computing the statistical features from the ultrasound image and finding optimally discriminant low-order speckle statistics. They succeeded in classifying regions as speckle or non-speckle by defining application-specific discriminant functions. Azar et al. [17] proposed a new combination of statistical features and explored their properties for speckle detection. These features were used as inputs to unsupervised clustering algorithms for the speckle classification. However, first-order statistics contain information only about the intensity values and the gray level distribution of the image, not about the pixel neighbourhood relationships. Therefore, the statistic features for two different windows (one with a speckle pattern, the other with a non-speckle pattern) with similar first-order histograms are indistinguishable. As a solution, second-order features derived from the co-occurrence matrix can represent this spatial relationship between pixels. These features include angular second moment, correlation, contrast and entropy, also known as Haralick features [18]. In [19] and [20], Wagner et al. evaluated second-order statistics for detecting and classification of speckle texture in diagnostic ultrasound. Carmo et al. [21] assessed the performance of several speckle detection methods that employed co-occurrence matrices for B-mode images. Widynski et al. [14] proposed a method for speckle spot detection using a morphological tree representation. They used detected speckle spots as markers for speckle tracking.

As shown in the result section, existing methods are not sufficient for automatic detection of suitable nodes, which is mainly because of two reasons: first, speckle patterns are complicated; therefore, it is not easy to model them based on some first and second-order features, second, mostly the information in the consecutive frame for detecting trackable speckles has been neglected. Moreover, Brynolfsson et al. [22] reported that Haralick features are sensitive to the image data. The result is highly dependent on parameter settings such as noise,

resolution and number of gray levels.

Since deep learning has been recently used as a powerful alternative for ultrasound image enhancement, segmentation and speckle reduction [23-25], it seems interesting to employ convolutional neural networks in speckle detection applications. Although numerous advanced techniques have been proposed for ultrasound speckle reduction [23-26], many studies on speckle detection based on ultrasound B-mode images are limited [11,21].

This study proposes a convolutional neural network (CNN) with a specialized structure for detecting trackable speckle spots, which can be employed in ultrasound speckle tracking applications. Specifically, we are interested in regions where speckle pattern has more properties of texture and stability over time, making them useful for tracking. The proposed network is able to classify a region of interest into two categories of trackable-speckle and non-trackable patterns. It should be noted that a region is defined as a squared window, and a node is placed at the centre of the window.

In order to find the optimal network, several CNNs with different configurations were trained and tested on a labelled dataset, including about 29500 image patches of ultrasound trackable-speckle and non-trackable patterns. To evaluate the network's performance, a comprehensive comparison between the proposed method and the existing methods, i.e. combination of feature extraction and supervised learning methods, was conducted. In order to investigate the applicability of the proposed method in speckle tracking, in silico experiments were conducted and compared with the state-of-the-art methods. The rest of the paper is organized as follows: In section 2, the concepts, methods and problems in speckle detection are briefly explained. In section 3, the proposed method is examined in detail. Section 4 explains the procedure of data preparation and conducting experiments. The results of the network-tuning and the evaluations are presented in section 5, and finally, section 6 concludes the study.

2.0 BACKGROUND

In this section, the importance and background of speckle detection are briefly explained. Specifically, the conventional approach for speckle detection is overviewed.

2.1 Speckle Detection

Speckles are also known as natural acoustic markers because they result from accumulating backscattered echoes from small elements in the tissue. Although they cannot exactly represent the structure of the tissue and are considered noises in some cases, speckles are highly correlated with the underlying microstructure of the tissue [11]. As a result, speckles within a window are usually stable and can be tracked when the associated region of the tissue moves [13,27].

A well-established algorithm for speckle tracking is block matching [28]. Considering that Frame A and Frame B are two consecutive frames in a sequence of echocardiograms, in the block matching technique, a window in frame a is compared with the neighbouring windows in frame b. The window with the highest matching score in frame b is considered the best match for the window in frame a. This selection is how we can tell that a tissue region is moved to a new position. In order to achieve accurate tissue tracking, the window in the frame should have a stable, trackable speckle pattern; otherwise, it leads to poor estimation of the new location. In other words, speckles with a similar topological structure over the next few frames are the best choices for speckle tracking. In this study, trackable speckle detection is a term that is used for examining whether a window has such a speckle pattern or not. Here, the window examined in speckle detection is called the target window. A window extracted from an image is also known as a patch.

In this study, the following criteria were considered as the underlying rule to classify the trackable speckle visually: "A batch of closely-connected speckles in a frame appears in the next frame with or without a geometric transformation, following a similar topology". Based on [14], the underlying definition of a speckle pattern is purely topological. Therefore, no assumption should be made about the intensity values.

2.2 Conventional Approach

A common technique for speckle detection usually uses feature extractors and machine learning models [11,17]. First, a set of statistical features is calculated for the target window. Then a decision is made to recognize the window either as trackable-speckle or non-trackable

patterns based on these values. Supervised classifiers can perform this categorizing task. It is worth mentioning that the performance of the speckle detector is highly dependent on the features and the supervised learning algorithm that we choose. Here, to compare our proposed model with conventional methods, the optimal combination of features and models is explained. A set of features suitable for speckle detection based on the first-order and second-order (specifically Haralick features [18]) statistics includes Mean, Variance, Skewness, Kurtosis, Angular Second Moment (ASM), Contrast, Correlation and Homogeneity [16,29]. Their mathematical formulas are described in Table 1. The first four measures can be calculated based on pixel intensity, while the rest should be computed using the co-occurrence matrix. A co-occurrence matrix (P) displays the frequency that two pixels with gray levels I1 and I2 appear in the window separated by a relative distance d in relative orientation θ [30]. Formally, given the image f with a set of G discrete intensity levels, the

matrix Pdθ(i, j) is defined such that its (i, j)th entry is equal to the number of times that

$$f(x1, y1) = i \; and \; f(x2, y2) = j \tag{1}$$

where

$$(x2, y2) = (x1, y1) + (d \cos\theta, d \sin\theta). \tag{2}$$

In the matrix $Pd\theta(i, j)$, i and j represent rows and columns, respectively.

A short description for each feature is as follows. The Mean represents the average level of intensity of the window being examined. The Variance measures how far the intensity values are spread out from the mean. Skewness and Kurtosis indicate the degree of histogram asymmetry around the mean and the histogram sharpness, respectively. ASM is also known as Energy which measures the smoothness of the image. The Contrast represents the local level of differences. The relation between pixels in two different directions is measured by Correlation. Finally, low-contrast images show high values for Homogeneity. Equation (2) indicates that changing d and θ results in different co-occurrence matrices and, consequently, several versions of Haralick features. Four angles of 0°, 45°, 90° and 135° are usually picked as the orientation θ. Since choices for d depends on the image parameters, e.g. texture, resolution and dimensions, three relative distances of $1px$, $3px$ and $7px$ were considered. In practice, for

each *d*, the resulting values for the four directions are averaged out. Thus, the total number of features extracted for each image patch in the dataset was sixteen.

Table 1. Mathematical description of selected first-order and second-order features

Feature	Formula
Mean(m)	$\sum_{x,y}^{M,N} \frac{f(x,y)}{M \times N}$
Variance(σ2)	$\sum_{x,y}^{M,N} \frac{(f(x,y)-m)^2}{M \times N}$
Skewness	$\sum_{x,y}^{M,N} \frac{(f(x,y)-m)^3}{M \times N \times \sigma^3}$
Kurtosis	$\sum_{x,y}^{M,N} \frac{(f(x,y)-m)^4}{M \times N \times \sigma^4}$
ASM	$\sum_{i,j} P(x,y)^2$
Contrast	$\sum_{i,j} \lvert i-j \rvert^2 + log\ P(x,y)^2$
Correlation	$\sum_{i,j} \frac{(i-\mu_i) \times (j-\mu_j)}{\sigma_i \times \sigma_j} \times P(i,j)$
Homogeneity	$\sum_{i,j} \frac{P(i,j)}{1+\lvert i-j \rvert^2}$

Note: μ_i, μ_j, σ_i and σ_j are the means and standard deviations of resulted vectors from summing the columns and rows of $P(i,j)$, respectively.

In the classification stage, three classifiers of K-Nearest Neighbor (KNN), Random Forest and AdaBoost were employed to label the image patch as trackable-speckle or non-trackable patterns based on the extracted features.

2.3 Problems

A conventional method has three major drawbacks that lead to poor trackable-speckle spot detection. The first one is the selection of texture features based on which building a precise model of the complex pattern of ultrasound speckles becomes difficult. The second one concerns that the initial parameters for feature calculation, e.g. d and θ, should be selected concerning the image's properties such as noise, resolution and texture. The conventional approach's last and most important problem is that it relies only on the target window and ignores the next frame's information for detecting a trackable pattern.

3.0 THE PROPOSED METHOD

This section introduces a convolutional neural network (CNN) with a novel architecture, called SpeckleDNet, to address the issues explained in section 2.3 for trackable speckle detection.

An important aspect of a CNN is that the feature extraction process is integrated into the network, not as a distinct but inseparable part from the learning process. This architecture lets the network to adaptively learn and extract the most discriminative features based on the relation between the inputs and outputs. Thus, SpeckleDNet inherently solves the problems of the conventional approach related to the selection of features. But the innovational aspect of SpeckleDNet is that it also takes advantage of the next frame because, as discussed in section 2.1, considering the next frame as a complementary source is beneficial for achieving higher performance in detecting trackable speckle spots.

The duty of SpeckleDNet is to correctly classify a target window into two categories of trackable-speckle or non-trackable patterns with the help of the complimentary window. As shown in Figure 1, the target window is a window in the frame meant to be classified, while the complementary window (patch) is the window in frame b that should be used as the extra information. Both windows have the same central position in the frames. Since the speckles within the target window might have a displacement between frames a and b, the size of the complementary window is considered twice the size of the target window to contain surrounding pixels. Since the network is trained with patches with different sizes, the size of the region of interest can be selected from 12×12 to 48×48 pixels. Therefore, the windows should be eventually resized to fit the dimensions of the corresponding input layer.

In order to process both the target and complementary windows, SpeckleDNet has a dual-path structure with two distinct input gates. As illustrated in Figure 2, the two pathways are called the main pathway and the complementary pathway. The main pathway itself is divided into two parts named primary-path and merge-path. The complementary pathway can be merged into the main pathway by concatenating the outputs of the complement pathway and the primary path together and feeding the concatenation result to the merge path. So, the output dimensions of the complement pathway and the primary path are the same. After running comprehensive experiments, the

optimal architecture for SpeckleDNet was fine-tuned as follows. The dimensions of the input layers are 30×30 and 40×40 pixels for the main and complementary pathways, respectively, which any user input image will be resized to. The main pathway starts with the primary part, which consists of two consecutive convolutional layers of Conv (3×3)×32 and Conv (3×3)×128, and one MaxPooling (3×3) layer. The complementary path includes a combination of convolution and pooling layers in the following order: Conv (3×3)×32, MaxPooling (2×2), Conv (3×3) ×64, Conv (3×3)×64 and MaxPooling (2×2). Through these two paths, the dimensions of the target and complementary windows are gradually reduced to the same size of 13×13 pixels. The outputs of the primary and complementary paths are concatenated to have a total of 192 feature maps which then are fed to the merge path. The merge path includes two consecutive convolutional layers of Conv (3×3)×32 and Conv (3×3)×128, one MaxPooling (3×3) layer, a fully connected layer with 512 neurons and finally one neuron as the output. For convolutional layers, the values in the parentheses show the dimensions of the filters, and the third value indicates the number of filters.

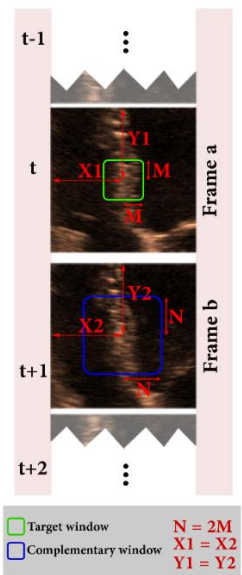

Figure 1: The target and complementary windows in two consecutive frames. It should be noted that the windows are shown relatively larger for presentation purposes.

A rectified linear unit is used as the activation function for the hidden layers. A sigmoid activation function is used for the output layer to have the occurrence probability of two classes. For each convolutional layer, a dropout rate of 0.3 is considered to minimize the overfitting effect. Based on the benchmark presented in [31], the Adam optimizer with a learning rate of 0.001 is an optimal choice for the network.

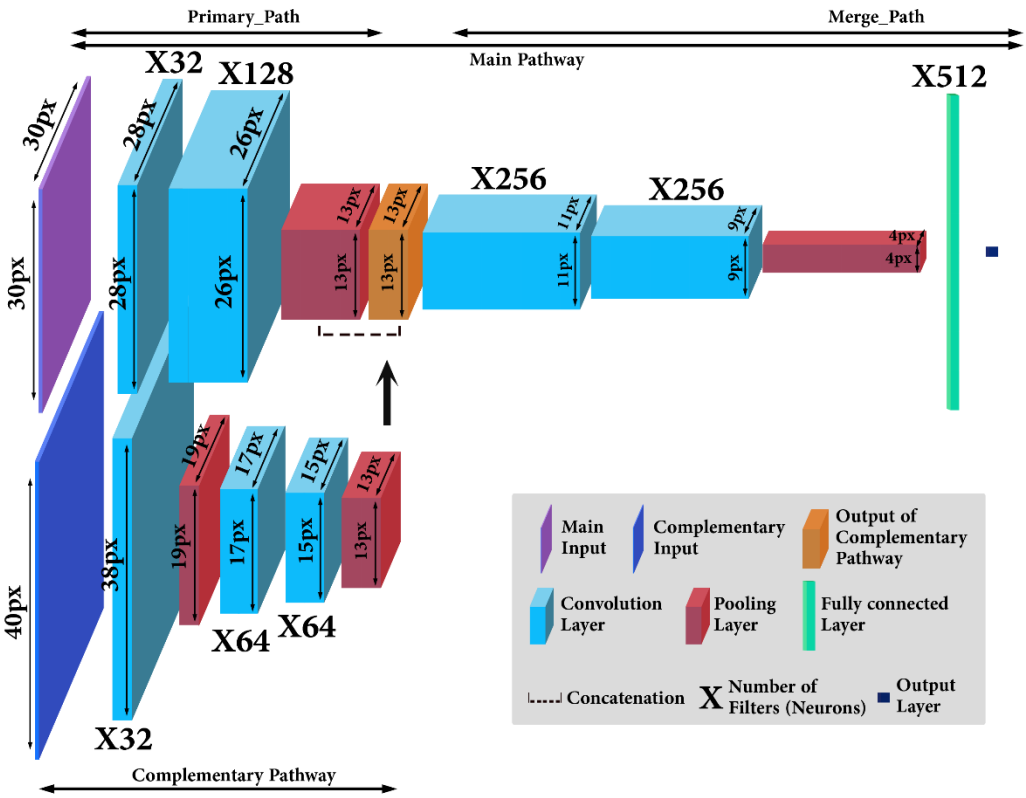

Figure 2: The target and complementary windows in two consecutive frames.

4.0 SETUP AND EXPERIMENTS

4.1 Data acquisition

Deep learning needs a huge amount of data to work [32]. In order to provide this study with a sufficient amount of data, echocardiographic sequences of 65 people were obtained with the help of expert cardiologists and in collaboration with Rajaie Cardiovascular Medical

& Research Center (RCMRC), Tehran, Iran. The subjects included males and females with both normal and ischemic cardiac conditions. Written informed consent for gathering this dataset was taken from all the subjects, and the study was approved by the ethics committee of RCMRC. The echocardiography was performed in all the three views of the apical 4-chamber, apical long-axis and parasternal short-axis for each subject. A clinical echocardiography ultrasound system (GE Vivid 7, GE Medical System, Milwaukee, Wisconsin, USA) with a 1.7 MHz phased array probe was used for this purpose. The sequences were captured with different frame rates between 42 and 68 with the size of 640×480 pixels. Based on the physical condition of each subject, different depths from 13 to 22 cm were considered for the echocardiography.

4.2 Dataset Preparation

A dataset including paired patches for main and complementary input gates was needed to feed and train the proposed network. Therefore, an average of 10 patches with different sizes ranging from 12×12 to 48×48 pixels were randomly extracted from each frame, except the last one, of all the sequences. Then, for each extracted target patch, its complimentary patch from the next frame was extracted with the same centre. As explained in Section 3, the size of the complementary patch in frame b was considered twice the size of its associated target patch in frame a. However, to feed the network, the patches were eventually resized to the dimensions of the corresponding input layer, i.e. 30×30 and 40×40 pixels for the main and complementary pathways. The most important part was manually labelling the paired patches as trackable-speckle or non-trackable. For this purpose, three experts in echocardiography performed annotating tasks based on the criterion classification explained in Section 2.1. Then, the consensus of the three experts was considered as the final labels.

Overall, the dataset was prepared with 15000, 3500 and 11000 (total 29500) samples for training, validation, and testing. The category distribution in each dataset was considered roughly balanced between the two classes. In order to have a reliable evaluation, patches for training, validation and testing were extracted from completely different subjects. Several samples from a total of 29500 extracted patches are shown in Figure 3. Subplots (a) and (b) display trackable-

speckle or non-trackable pattern samples that are considered as the target patches. Subplots (c) and (d) present the corresponding complementary patches extracted from the next frame for the samples in subplots (a) and (b), respectively.

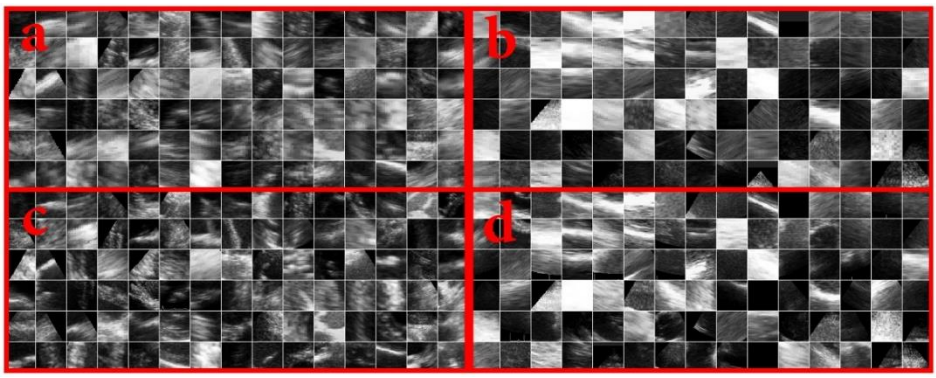

Figure 3: A few samples from a total of 29500 extracted patches. (a) and (b) display trackable-speckle and non-trackable samples. (c) and (d) present the corresponding complementary patches for the samples in subplots (a) and (b), respectively.

4.3 Implementation

SpeckleDNet was implemented in Python 3 using TensorFlow 2.0 and Keras framework. The source code is available for public usage at https://github.com/mitechworld/SpeckleDNet. A system with an Intel Core i7 CPU and 8 gigabytes of RAM was used to conduct the experiments. To increase the training speed, multicore processing on the CPU was also employed.

4.4 Metrics

In this study, categorizing a window as a trackable-speckle is considered a positive output. Thus, if a window truly contains a trackable-speckle pattern, it counts as a True Positive (TP) prediction. When the window has a non-trackable pattern but is categorized as a trackable-speckle, it should be considered a False Positive (FP) prediction. On the contrary, True Negative (TN)/False Negative (FN) represents the number of observations predicted correctly/wrongly as non-trackable. In speckle tracking, it is important to track only the windows with the trackable-speckle pattern even if the price is to ignore some of them. In other words, although the model should

correctly identify trackable-speckle windows as much as possible (decreasing the FN number), it is not preferred to tag a non-trackable window as a trackable-speckle (decreasing the FP number) because it eventually leads to a poor tracking result.

On the one hand, a metric is desired to demonstrate how much a model is good in assigning trackable-speckle labels only to those windows that are, in fact, with a trackable-speckle pattern. This can be measured by Precision which is formulated as (3). On the other hand, it is necessary to measure the general ability of a model in finding the trackable-speckle windows. Recall is a common metric for this purpose and is calculated based on (4). The optimal values for these metrics are achievable by changing the probability threshold of the classifier and plotting the precision-recall curve.

Overall, in order to evaluate a model with regard to both Precision and Recall, two popular measures are F1-score (5) and the area under the precision-recall curve (AUPRC). F1 measures the ability of a model for a specific probability threshold, whereas AUPRC summarizes the model's ability across thresholds.

$$Precision = \frac{TP}{TP + FP} \tag{3}$$

$$Recall = \frac{TP}{TP + FN} \tag{4}$$

$$F1 = 2\frac{Precision.Recall}{Precision + Recall} \tag{5}$$

4.5 The procedure of tuning CNN Parameters

To find the optimal parameters for the network and achieve the proposed model, i.e. SpeckleDNet, several network structures through grid search were carefully trained and tested on the train and validation datasets, respectively. Grid search is a hyper-parameter tuning method in which different parameters are considered to find the optimal combination of values for the network. All the networks were compared based on their AUPRC score for tuning the parameters. As discussed in Section 3, the proposed network has a dual-path structure that includes the main and complementary pathways. Therefore, the parameters were first tuned for the main pathway alone, and then they

were adjusted for the complementary pathway considering the configured main pathway.

In the first series of experiments, a single-path structure was the subject of inquiry to find the optimal dimensions of the input layer, the number of layers and filters for the main path. Table 2 contains three networks with different numbers of layers where w is a coefficient for the number of filters. Accordingly, different numbers of filters were generated by assigning selected values of 10, 16 and 22 to the coefficient w. After finding the structure with the optional number of layers and filters, dimensions between 14×14 and 46×46 were tested as the input size for the elected structure.

Table 2: Three candidate structures for the main pathway

Number of convolution layers	Structure
3	Conv(3× 3)× 2w, Conv(3×3)×4w, MaxPooling(2×2), Conv(3×3)×16w, FC×32w
4	Conv(3× 3)× 2w, Conv(3×3)×4w, MaxPooling(2×2), Conv(3×3)×8w, Conv(3×3)×16w, MaxPooling(2×2), FC×32w
5	Conv(3× 3)× 2w, Conv(3×3)×4w, MaxPooling(2×2), Conv(3×3)×8w, Conv(3×3)×8w, MaxPooling(2×2), Conv(3×3)×16w, MaxPooling(2×2), FC×32w

Note: w is the coefficient for the number of filters.

The second series of experiments concerned the complementary path with regard to the chosen main pathway. As shown in Table 3, three structures with a different number of layers were examined to find the optimal combination of convolution and pooling layers. Considering that the output dimensions of the complementary pathway should be the same as the primary pathway's, the input size for a particular structure was fixed. Similar to the first series of

experiments, coefficient w was replaced by 10, 16 and 22 to generate different numbers of filters. The results of these experiments are presented in Section 5.1.

Table 3. Three candidate structures for the complementary pathway

Number of convolution layers	Structure
2	Conv(3× 3)× 2w, MaxPooling(2×2), Conv(3×3)×4w
4	Conv(3× 3)× 2w, MaxPooling(2×2), Conv(3×3)×4w, Conv(3×3)×4w, Conv(3×3)×4w
6	Conv(3× 3)× 2w, MaxPooling(2×2), Conv(3×3)×4w, Conv(3×3)×4w, Conv(3×3)×4w, Conv(3×3)×4w, Conv(3×3)×4w

Note: w is the coefficient for the number of filters.

4.6 Comparing SpeckleDNet with a conventional approach

A set of experiments were conducted to compare the classification results of SpeckleDNet and the conventional approaches (which consist of two parts of feature extraction and classification). As explained in Section 2.2, a combination of sixteen features and three classifiers were selected, which are used as the conventional method. In order to have a fair comparison, the conventional methods were evaluated on the same dataset as for SpeckleDNet. All the methods were compared based on Precision, Recall and F1 scores.

4.7 Evaluation of SpeckleDNet in speckle tracking

In this set of experiments, the goal was to investigate the impact of the proposed speckle detection method in speckle tracking and compare it with others. For this purpose, a synthetic database generated and explained by [33,34] was used. This dataset consists of 8 synthetic ultrasound sequences. The simulated sequences appear similar to real ultrasound recordings, yet, the myocardial motion is fully controlled

by the electromechanical (E/M) model in [35]. Therefore, it is a feasible alternative for the evaluation of different speckle tracking applications because we can calculate the accuracy of displacement estimation based on the ground truth data. In fact, in the simulated model, we have access to the nodes and their positions in each frame. In order to evaluate speckle tracking accuracy, a window around a node is first selected and then tracked over the consecutive frames. The error between the estimated position and the ground truth position shows the accuracy of speckle tracking. However, as explained earlier, not every node is suitable for tracking, and it could lead to a miscalculation of displacements. Therefore, a set of suitable nodes for tracking were chosen using the proposed speckle detection network, and only those nodes were tracked. The overall error was compared with the case in which the same number of nodes were chosen randomly for tracking. To achieve a more reliable conclusion, the process was repeated with a different number of nodes, and the errors were averaged at the end. The results are explained in section 5.

5.0 RESULTS AND DISCUSSION

5.1 Choosing the parameters of SpeckleDNet

Based on the procedure in Section 4.5, several network structures were carefully tested to find the best hyper-parameters for the proposed SpeckleDNet. The result of trying different numbers of layers and filters for the main path is shown in Figure 4, from which it is understandable that increasing the number of layers and filters did not necessarily lead to better performance. Based on the maximum AUPRC of 0.963, the 4-layer architecture with the filter coefficient w=16 was selected for the main path. For the selected structure, the AUPRC scores of 0.947, 0.958, 0.964, 0.955 and 0.949 were recorded for different dimensions of 14×14, 22×22, 30×30, 38×38 and 46×46 pixels, respectively. The result illustrates that enlarging the input size might cause an improvement but only to a certain point after which the performance decreases. Therefore, the dimensions of 30×30 pixels with a maximum score of 0.964 were considered the optimal window size for the main pathway input.

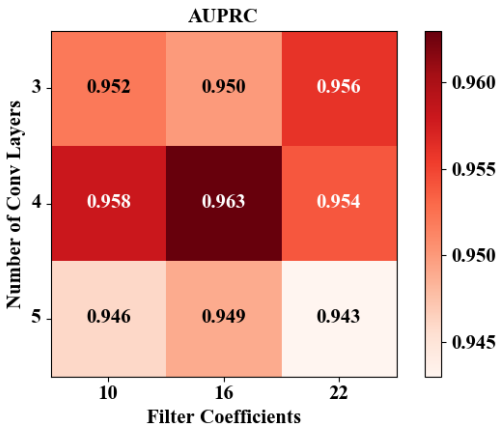

Figure 4: The result of trying different numbers of layers and filters for the main path.

Similarly, the best configuration for the complementary path was selected from nine candidate networks whose AUPRC scores are shown in Figure 5. The structure with four layers and the filter coefficient w=10 achieved the maximum score of 0.978. Based on the selected structure and the desired output size, there was no choice but to consider the input size as 40×40 pixels for the complementary pathway. With this configuration, the total number of trainable parameters for the proposed network reached 3,063,489.

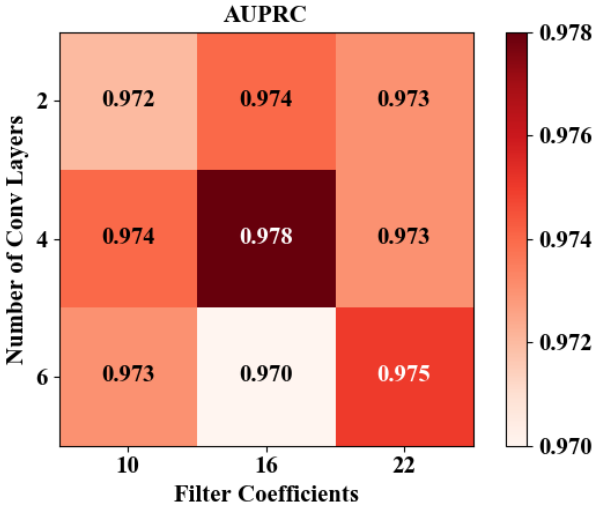

Figure 5: The result of trying a different number of layers and filters for the complementary path.

Comparing the results of the single-path structure with the dual-path structure reveals that using the complementary pathway led to an increase in the AUPRC score. It demonstrates that using the information in the next frame was beneficial for trackable speckle detection.

5.2 Performance of SpeckleDNet

The proposed method in this study for trackable speckle detection was compared with three common methods in terms of precision, recall, F1-score and accuracy. The results are presented in Table 4. It is obvious that the proposed CNN network with the F1-socre of 0.9484 outperforms the random forest method, which earned the best F1-score (0.8910) in comparison to KNN (0.8591) and AdaBoost (0.8769). The same conclusion can be made based on the accuracy score as well. SpeckleDNet achieved an accuracy of 94.60% in trackable speckle detection while the other three methods achieved the maximum accuracy of 88.56%.

Table 4. Comparison between the proposed method and three common methods for trackable speckle detection

	First-order and second-order features +			
	KNN	Random forest	AdaBoost	**SpeckleDNet**
Precision	0.8121	0.8718	0.8535	**0.9316**
Recall	0.9119	0.9110	0.9016	**0.9658**
F1 score	0.8591	0.8910	0.8769	**0.9484**
Accuracy	0.8465	0.8856	0.8701	**0.9460**

5.3 Performance of SpeckleDNet

The averaged error of displacement estimation was calculated as 7.16 mm ± 1.02 mm (mean error ± std) for the case in which all the nodes were selected by our proposed method. In comparison, for randomly selected nodes, it was calculated as 9.49 mm ±0.49 mm. The p-value, calculated as 0.00066 ("0.05), shows that the performance is significant.

6.0 CONCLUSION

This study introduces a customized convolutional neural network with a dual-path structure named SpeckleDNet for speckle detection. The

network was trained and evaluated on a dataset with 29500 ultrasound image patches of trackable-speckle or non-trackable patterns. The results showed that the proposed CNN-based method performs considerably better than the existing methods. The F1-score and accuracy of SpeckleDNet earned the maximum values of 0.9484 and 94.60% among all the methods. So, it is recommended that SpeckleDNet be used instead of the conventional methods to achieve a more accurate trackable speckle detection system.

7.0 REFERENCES

[1] C Moran, Carmel M., and Adrian JW Thomson. "Preclinical ultrasound imaging—A review of techniques and imaging applications." Frontiers in Physics 8 (2020). DOI 10.3389/fphy.2020.00124

[2] Huang, Q., Zeng, Z.: A review on real-time 3d ultrasound imaging technology. Biomed Res Int 2017, 6027029 (2017). DOI 10.1155/2017/6027029.

[3] Rix, A., Lederle, W., Theek, B., Lammers, T., Moonen, C., Schmitz, G., Kiessling, F.: Advanced ultrasound technologies for diagnosis and therapy. J Nucl Med 59(5), 740–746 (2018). DOI 10.2967/jnumed.117.200030.

[4] Perperidis, A.: Postprocessing approaches for the improvement of cardiac ultrasound b-mode images: A review. IEEE Trans Ultrason Ferroelectr Freq Control 63(3), 470–85 (2016). DOI 10.1109/TUFFC.2016.2526670.

[5] Aubert R, Venner C, Huttin O, Haine D, Filippetti L, Guillaumot A, Mandry D, Marie PY, Juilliere Y, Chabot F, Chaouat A. Three-dimensional echocardiography for the assessment of right ventriculo-arterial coupling. Journal of the American Society of Echocardiography, 31(8), 905-15 (2018). DOI 10.1016/j.echo.2018.04.013

[6] Cameli, M., Mondillo, S., Solari, M., Righini, F.M., Andrei, V., Contaldi, C., De Marco, E., Di Mauro, M., Esposito, R., Gallina, S., Montisci, R., Rossi, A., Galderisi, M., Nistri, S., Agricola, E., Mele, D.: Echocardiographic assessment of left ventricular systolic function: from ejection fraction to torsion. Heart Fail Rev 21(1), 77–94 (2016). DOI 10.1007/s10741-015-9521-8.

[7] Shiri, M., Gifani, P., Behnam, H., Sani, Z.A., Yeganegi, H., Shojaeifard, M.: A color-encoded map to facilitate the identification of abnormal segments of the left ventricle by novice examiners. In: 2019 27th Iranian Conference on Electrical Engineering (ICEE), pp. 1737–1741 (2019). DOI

10.1109/IranianCEE.2019.8786695

[8] Amzulescu, M.S., De Craene, M., Langet, H., Pasquet, A., Vancraeynest, D., Pouleur, A.C., Vanoverschelde, J.L., Gerber, B.L.: Myocardial strain imaging: review of general principles, validation, and sources of discrepancies. Eur Heart J Cardiovasc Imaging 20(6), 605–619 (2019). DOI 10.1093/ehjci/jez041.

[9] Joos, P., Poree, J., Liebgott, H., Vray, D., Baudet, M., Faurie, J., Tournoux, F., Cloutier, G., Nicolas, B., Garcia, D., Baudet, M., Tournoux, F., Joos, P., Poree, J., Cloutier, G.,Liebgott, H., Faurie, J., Vray, D., Nicolas, B., Garcia, D.: High-frame-rate speckle-tracking echocardiography. IEEE Trans Ultrason Ferroelectr Freq Control 65(5), 720–728 (2018). DOI 10.1109/TUFFC.2018.2809553.

[10] Bansal, M., Kasliwal, R.R.: How do i do it? speckle-tracking echocardiography. Indian Heart J 65(1), 117–23 (2013). DOI 10.1016/j.ihj.2012.12.004.

[11] Damerjian, V., Tankyevych, O., Souag, N., Petit, E.: Speckle characterization methods in ultrasound images – a review. Irbm 35(4), 202–213 (2014). DOI 10.1016/j.irbm.2014.05.003

[12] Leitman, M., Lysyansky, P., Sidenko, S., Shir, V., Peleg, E., Binenbaum, M., Kaluski, E., Krakover, R., Vered, Z.: Two-dimensional strain-a novel software for real-time quantitative echocardiographic assessment of myocardial function. J Am Soc Echocardiogr 17(10), 1021–9 (2004). DOI 10.1016/j.echo.2004.06.019.

[13] Muraru, D., Niero, A., Rodriguez-Zanella, H., Cherata, D., Badano, L.: Three-dimensional speckle-tracking echocardiography: benefits and limitations of integrating myocardial mechanics with three-dimensional imaging. Cardiovasc Diagn Ther 8(1), 101–117 (2018). DOI 10.21037/cdt.2017.06.01.

[14] Widynski, N., G'eraud, T., Garcia, D.: Speckle spot detection in ultrasound images: Application to speckle reduction and speckle tracking. In: 2014 IEEE International Ultrasonics Symposium, pp. 1734–1737 (2014). DOI 10.1109/ULTSYM.2014.0430

[15] Prager, R.W., Gee, A.H., Treece, G.M., Berman, L.H.: Analysis of speckle in ultrasound images using fractional order statistics and the homodyned k-distribution. Ultrasonics 40(1-8), 133–137 (2002). DOI 10.1016/s0041-624x(02)00104-x

[16] Marti, R., Marti, J., Freixenet, J., Zwiggelaar, R., Vilanova, J.C., Barcelo, J.: Optimally discriminant moments for speckle detection in real b-scan images. Ultrasonics 48(3), 169–81 (2008). DOI 10.1016/j.ultras.2007.11.010.

[17] Azar, A.A., Rivaz, H., Boctor, E.: Speckle detection in ultrasonic images using unsupervised clustering techniques. Conf Proc IEEE Eng Med Biol Soc 2011, 8098–101 (2011). DOI 10.1109/IEMBS.2011.6091997.

[18] Haralick, R.M., Shanmugam, K., Dinstein, I.: Textural features for image classification. IEEE Transactions on Systems, Man, and Cybernetics SMC-3(6), 610–621 (1973). DOI 10.1109/tsmc.1973.4309314

[19] Wagner, R.F., Smith, S.W., Sandrik, J.M., Lopez, H.: Statistics of speckle in ultrasound b-scans. IEEE Transactions on Sonics and Ultrasonics 30(3), 156–163 (1983). DOI 10.1109/t-su.1983.31404

[20] Wagner, R.F., Insana, M.F., Brown, D.G.: Unified approach to the detection and classification of speckle texture in diagnostic ultrasound. Opt Eng 25(6), 738–742 (1986). DOI 10.1117/12.7973899.

[21] Carmo, B.S., Prager, R.W., Gee, A.H., Berman, L.H.: Speckle detection for 3d ultrasound. Ultrasonics 40(1-8), 129–132 (2002). DOI 10.1016/s0041-624x(02)00101-4

[22] Brynolfsson, P., Nilsson, D., Torheim, T., Asklund, T., Karlsson, C.T., Trygg, J., Nyholm, T., Garpebring, A.: Haralick texture features from apparent diffusion coefficient (adc) mri images depend on imaging and pre-processing parameters. Sci Rep 7(1), 4041 (2017). DOI 10.1038/s41598-017-04151-4.

[23] Abdel-Nasser, M., Omer, O.A.: Ultrasound image enhancement using a deep learning architecture. In: A.E. Hassanien, K. Shaalan, T. Gaber, A.T. Azar, M.F. Tolba (eds.) Proceedings of the International Conference on Advanced Intelligent Systems and Informatics 2016, pp. 639–649. Springer International Publishing (2016). DOI 10.1007/978-3-319-48308-561

[24] Hyun, D., Brickson, L.L., Looby, K.T., Dahl, J.J.: Beamforming and speckle reduction using neural networks. IEEE Trans Ultrason Ferroelectr Freq Control 66(5), 898–910 (2019). DOI 10.1109/TUFFC.2019.2903795.

[25] Dietrichson, F., Smistad, E., Ostvik, A., Lovstakken, L.: Ultrasound speckle reduction using generative adversial networks. In: 2018 IEEE International Ultrasonics Symposium (IUS), pp. 1–4 (2018). DOI 10.1109/ULTSYM.2018.8579764

[26] Joel, T., Sivakumar, R.: An extensive review on despeckling of medical ultrasound images using various transformation techniques. Applied Acoustics 138, 18–27 (2018). DOI 10.1016/j.apacoust.2018.03.023

[27] Badano, L.P., Kolias, T.J., Muraru, D., Abraham, T.P., Aurigemma, G., Edvardsen, T., D'Hooge, J., Donal, E., Fraser, A.G., Marwick, T. and

Mertens, L. Standardization of left atrial, right ventricular, and right atrial deformation imaging using two-dimensional speckle tracking echocardiography: a consensus document of the EACVI/ASE/Industry Task Force to standardize deformation imaging. European Heart Journal-Cardiovascular Imaging, 19(6), pp.591-600 (2018). DOI 10.1093/ehjci/jey042

[28] Yaakob, R., Aryanfar, A., Halin, A.A., Sulaiman, N.: A comparison of different block matching algorithms for motion estimation. Procedia Technology 11, 199–205 (2013). DOI 10.1016/j.protcy.2013.12.181

[29] Molinari, F., Caresio, C., Acharya, U.R., Mookiah, M.R., Minetto, M.A.: Advances in quantitative muscle ultrasonography using texture analysis of ultrasound images. Ultrasound Med Biol 41(9), 2520–32 (2015). DOI 10.1016/j.ultrasmedbio.2015.04.021.

[30] Baek, J., Poul, S.S., Swanson, T.A., Tuthill, T. and Parker, K.J. Scattering signatures of normal versus abnormal livers with support vector machine classification. Ultrasound in Medicine & Biology, 46(12), pp.3379-3392 (2020). DOI 10.3390/e22050567

[31] Schneider, F., Balles, L., Hennig, P.: Deepobs: A deep learning optimizer benchmark suite. arXiv preprint arXiv:1903.05499 (2019)

[32] Razzak, M.I., Naz, S., Zaib, A.: Deep Learning for Medical Image Processing: Overview, Challenges and the Future, pp. 323–350. Springer International Publishing, Cham (2018). DOI 10.1007/978-3-319-65981-7 12. URL https://doi.org/10. 1007/978-3-319-65981-7_12

[33] Alessandrini, M., De Craene, M., Bernard, O.: A pipeline for the generation of realistic 3d synthetic echocardiographic sequences: Methodology and open-access database. IEEE Trans Med Imaging 34(7), 1436–1451 (2015). DOI 10.1109/TMI.2015.2396632

[34] Alessandrini, M., Heyde, B., Queiros, S.: Detailed evaluation of five 3d speckle tracking algorithms using synthetic echocardiographic recordings. IEEE Trans Med Imaging 35(8), 1915–1926 (2016). DOI 10.1109/TMI.2016.2537848

[35] Marchesseau, S., Delingette, H., Sermesant, M., Sorine, M., Rhode, K., Duckett, S., Rinaldi, C., Razavi, R., Ayache, N.: Preliminary specificity study of the bestel–cl'ement–sorine electromechanical model of the heart using parameter calibration from medical images. Journal of the Mechanical Behavior of Biomedical Materials 20, 259 – 271 (2013). DOI https://doi.org/10.1016/j.jmbbm.2012.11.021.

ARTIFICIAL INTELLIGENCE IN MOTOR IMAGERY-BASED BCI SYSTEMS: A NARRATIVE REVIEW

S.F. Nasim[1]*, S. Fatimah[1] and A. Amin[2]

[1]Department of Computer Science and IT, NED University of Engineering & Technology, 75270, Karachi, Sindh, Pakistan.

[2]Department of Computer Science and Engineering, NED University of Engineering & Technology, 75270, Karachi, Sindh, Pakistan.

*Corresponding Author's Email: sfaizaadnan@gmail.com

Article History: Received April 16, 2022; Revised May 17, 2022; Accepted May 25, 2022

ABSTRACT: Artificial intelligence concepts using machine learning models are implemented in medicines to examine medical data and gain insights to improve decision-making. This paper provides a narrative review of "Motor Imagery based brain-computer interface systems". The essential techniques of machine learning and deep learning are reviewed and compared based on computation and test data accuracy. Various preprocessing and feature extraction techniques are highlighted in this paper, which include FFT-LDA, Wavelet Packet Decomposition (WPD), CSP Algorithm, Fisher ratio algorithm, Discrete Wavelet Transform, and Filter Bank Common Spatial Pattern (FBCSP). This method collects outcomes with multiple perspectives of the MI-BCI and optimizes it. Necessary details of Algorithms applied are also compared to give an insight into Ml techniques.

KEYWORDS: *EEG signal, Motor imagery (MI), Fourier transform (FFT), Classification Models.*

1.0 INTRODUCTION

The Brain-computer interface is a technique that decodes brain activity based on EEG signals. It is a system that creates a direct link between the human brain and the computer, allowing the tasks to be performed without using muscles and peripheral nerves. BCI system creates a device that makes individuals control the automated systems without

using muscles but rather completely by thoughts. An electroencephalogram or Brain computer-based system measures specific features of an individual's brain signal, which correlates with their intention to affect control. [12] The system then translates such features into control signals to control external devices. Such technology is especially used in the medical field for neuro-muscular disorder patients, such as patients with "Amyotrophic Lateral Sclerosis (ALS), brainstem stroke, brain or spinal cord injury, cerebral palsy, muscular dystrophies, and multiple sclerosis". [15]

One of the most used methods to record the brain's electrical activity is EEG. It requires electrodes to be placed on the individual's scalp to capture brain waves quickly and with high temporal resolution. However, most studies show that it also has a high noise level and low spatial resolution, making extracting useful information from EEG signals challenging for BCI systems. [15]

The condition of cerebral mental processing in which an individual models a physical activity or stimulates a motor action is known as motor imagery (MI). MI is the mental repetition of a motor act, such as "leg motions, tongue movements, hand movements, and finger movements", without any clear motor activity. BCI has made extensive use of MI. According to a research, it has been observed that the impact of MI training on learning and holding a foot sequence task has been explored already with thirty right-footed subjects between the ages of 22 and 37 years (mean: 27.4 ± 4.1 years) and randomly assigned to one of three groups, as it practised a serial response time task with a sequence of three dorsal flexions and three plantar flexions with the left foot.MI training works to develop motor performance, and that mental implementation may induce nonspecific effects as well.

For recording motor imaginary brain activity, various acquisition strategies are available. Because of its high temporal resolution, non-invasiveness, simplicity of installation, and low start-up costs, EEG is the most investigated possibility for non-invasive interface BCI designs. The scientists predicted that a good model of this occurrence might be employed as a valid character in categorization by visualizing a mental exercise. MI categorization is a tough and delicate topic since EEG recordings have a poor signal-to-noise ratio (SNR) and contain undesirable information such as artefacts. Signals that are not considered in ML algorithms in the main signal can be termed noise, artefacts, or interference. To remove noise in ML preprocessing steps will be applied in order to get clean data set, so there will o early

stopping in ML. To solve these issues, MI classification has also attracted several researchers. In this paper, we will analyze different feature extraction methods from EEG signals and propose a collection of methods that provide improved results for EEG-based motor imagery classification.

2.0 MATERIALS AND METHODS

The BCI system relies on pattern recognition. As a result, multiple research papers have looked at different classification and feature extraction methodologies and methods for MI task recognition. [4] The overall block diagram for the process is shown in Fig 1 and is concluded by reviewing different research papers.

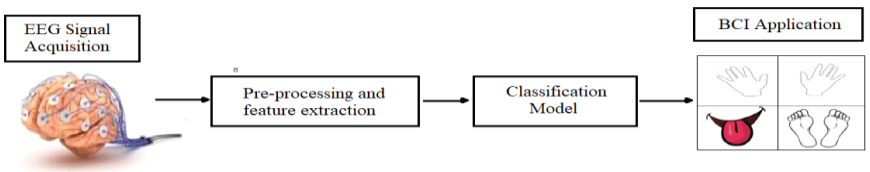

Fig 1: Feature Extraction

All the studies incorporated EEG signals with different data acquisition methods in their research. Table 1 includes the difference between the collected data sets of the studies:

3.0 RESEARCH METHODS

Preprocessing of acquired signals is necessary to reduce any noise or artefacts captured during the acquisition process. [4] These undesirable signals include the interference created when the device is mounted on the individual, EMG signals resulting from muscular contractions, and ocular artefact resulting from eye movement or blinking. This undesired noise in the EEG dataset will cause misinterpretation of the findings and incorrect conclusions; thus, they shall be filtered. The most used preprocessing method is using bandpass filters.

The identification of patterns is an essential component of the BCI system. This process is necessary because the EEG data set is typically

very large; that is, it may contain 250-time samples per second of EEG data leading to indiscriminate differences between distinct MI orders in the EEG signal, feature extraction is required.

This process aims to filter the raw EEG data signals from the unwanted background noise. [4] The EEG signals are divided into different frequency bands such as "alpha, delta, beta, gamma, and theta" bands. The frequency range of motor imagery lies within the alpha or beta band range. Hence, the signal processing of EEG signals should be processed in terms of frequency. Fourier transform (FFT) is applied to convert raw time-domain EEG signals into the frequency domain. Table 2 shows the chart of several preprocessing and feature extraction techniques explored by various researchers for MI task recognition.

Table 1: EEG signals data

Year Published	EEG Acquisition	No of the Participants in MI	MI Tasks:	No of Trials per Movement
March 2019	Dataset from "BCI Competition IV provided by B.Blankertz , C. Vidaurre, and K.-R. Müller from Berlin" was used	4 (healthy)	Hand movements, Foot movement	100
December 2020	BCI competition IV-2a	9 (Healthy)	Eyes open, eyes closed, Eye movement, Foot movement	72
December 2020	Multichannel EEG amplifiers with 64 channels were used to record EEG	5 (healthy)	Six different combinations of hands and feet movements.	60
June 2021	The Emotiv headset was used to collect the EEG dataset.	42	Hands movements, Feet Movements, Tongue movements, Eye movement	48
July 2021	Sixteen electrodes headset was used to record EEG signals per 10-20 intl. system.	57	Eye movements, Hand Movements	120

Isa et al. (2018) suggested applying "Linear Discriminant Analysis (LDA)" to the features obtained from FFT in order to develop better computational efficiency of the AI model. LDA reduces the number of

dimensions in a dataset resulting in the optimization of class separability by finding the feature subspaces. This method also reduces the chances of overfitting the data set.

However, Zheng et al. (2020) suggested an algorithm for feature extraction using transfer learning. This algorithm solves the long calibration time problem and lack of MI commands and increases the accuracy of the model. Because Spatial filters are used in feature extraction, making the algorithm more physiologically plausible in poor performers. Transferring source data from the old MI command makes this algorithm capable of performing efficiently for fewer training samples of the new MI command. However, this method is only suitable for discriminating between two classes [12].

Table 2: Preprocessing/feature extraction techniques

Year Published	**Preprocessing techniques**	**Feature Extraction Methods**
March 2019	Not Applied	FFT-LDA feature extraction
December 2020	EOG interference noise was removed. To increase SNR, EEG signals were filtered through the "Butter-worth" bandpass filter	"Wavelet Packet Decomposition (WPD)" method and "spatial characteristics using the Common Spatial Pattern (CSP)" method
December 2020	Noise caused by muscle movement and bias was removed by the Reference method. Dataset was filtered through a bandpass filter	CSP Algorithm and Fisher ratio algorithm
June 2021	Each channel was resampled to 128 Hz, and the dataset was filtered through a low pass filter.	Method of "Discrete Wavelet Transform with Maximum Overlap"
July 2021	The data set was filtered for the ML model but not for the DL model	"Filter Bank Common Spatial Pattern (FBCSP)" method

"Discrete Wavelet Transform with Maximum Overlap" method was suggested by Abdul Wahab (2021) to categorize the theta and delta patterns of very low and high frequencies of brain activities during mediation, learning, sleeping or focus mode. According to him, "in MODWT, the relative tolerance is independent of the detailed elements but can change when approximation or detail elements change".

4.0 RESULTS

In this paper, classification is the technique applied to identify different sample classes in the data set. For motor imagery, different classes are a form of movement involving the left and right hands, the feet, and the eyes. To classify the MI signals, machine learning is widely used. But in recent years, more attention to the development of deep learning resulted in CNN and ANN-based classification models for motor imagery BCI systems. Table 3 shows the comparison chart of several studies and their resulting outcomes.

5.0 CONCLUSION

For a BCI system to work ideally for all the users, it is critical to develop a "classification" model that can differentiate task-related patterns of each individual with high accuracy. This article reviewed various research improving the effectiveness of machine learning techniques in Motor imagery-based BCI systems and deep learning needs in enhancing the motor imagery BCI system's performance (Table 3). By comparing the results and accuracies of all the models on test data, it is found that the task transfer learning method works best for feature extraction. This algorithm solves the long calibration time problem and lack of MI commands and increases the accuracy of the model.

The SVM classifier yields the best results out of all the ML algorithms. However, the highest level of accuracy was attained with the CNN model, which outperformed all the ML classification models and ANN model. The CNN model is also trained and tested for raw data; thus, it eliminates the need for preprocessing and feature extraction but requires a large data set. In conclusion, deep learning classifiers have more potential MI-BCI apps for all users in the future. This situation is contrasts with ML-based BCI systems, which need a significant amount of feature extraction and preprocessing yet are prone to inaccuracies and are not suitable for some users.

Table 3: Comparative Studies

Year Published	Algorithm applied	Necessary detail	AI Feature	Outcomes	Metrics/ Reference type
March, 2019	Classification	Classifiers: SVM, k-NN, Naïve Bayes, Decision Tree, Logistic Regression	ML	When compared to accuracy measurement, the area under the curve measurement yields a better result with "SVM, Logistic Regression, and the Naïve Bayes classifier" producing the best results with an accuracy of 89.09%"	Accuracy, AUC
December 2020	ANN CNN	Activation functions for ANN: Relu, Selu, Elu, tanh Activation function for CNN: Softmax	DL	ANN and CNN are both comparable as running classification on test data from 22 EEG channels yields the accuracy of 82.93% with CNN and 81.03% with ANN	Accuracy
December 2020	Classification	SVM classifier with "Gaussian radial basis function" as the kernel function	ML	The algorithm performs better, especially for datasets with fewer training samples and poor performance.	Accuracy
June, 2021	Classification	SVM classifier with several kernel functions	ML	The average accuracy achieved for SVM is 98.81%, with cubic SVM yielding the highest results with an accuracy of 97.77%	Accuracy
July 2021	Classification CNN	LDA classifier 2D CNN model with Relu as an activation function	ML DL	The average test accuracy of the CNN model is greater than CSP+LDA classifiers, and it outperformed CSP+LDA by 18.38% as per the t-test.	Accuracy Pairwise t-test

6.0 ACKNOWLEDGEMENT

Finally, it is a real pleasure for me to acknowledge the contributions of my amazing partner Sana Fatima who's working with me at NED University as a Lecturer, as well as Areeba, my student who is enrolled in Ned University CIS department; both of them gave up their time and read every version of this paper.This paper and the research behind it would not have been possible without their extraordinary support. We worked to provide valuable insight into FOD deduction using AI techniques and compare various techniques as well.

7.0 REFERENCES

[1] N. Tibrewal, N. Leeuwis and M. Alimardani, "The Promise of Deep Learning for BCIs: Classification of Motor Imagery EEG using Convolutional Neural Network", *biorxiv.org*, 2021. [Online]. Available: https://www.biorxiv.org/content/10.1101/2021.06.18.448960v1.full. [Accessed: 23- Feb- 2022].

[2] N. Md Isa, A. Amir, M. Ilyas and M. Razalli, "Motor imagery classification in Brain computer interface (BCI) based on EEG signal by using machine learning technique". *Bulletin of Electrical Engineering and Informatics*, vol. 8, no. 1, pp. 269-275, 2019. Available: 10.11591/eei.v8i1.1402 [Accessed 23 February 2022].

[3] Akrout, A. Echtioui, R. Khemakhem and M. Ghorbel, "Artificial and Convolutional Neural Network of EEG-Based Motor imagery classification: A Comparative Study", *2020 20th International Conference on Sciences and Techniques of Automatic Control and Computer Engineering (STA)*, 2020. Available: 10.1109/sta50679.2020.9329317 [Accessed 23 February 2022].

[4] S. Abdulwahab, H. Khleaf and M. Jassim, "EEG Motor-Imagery BCI System Based on Maximum Overlap Discrete Wavelet Transform (MODWT) and Machine learning algorithm", *Iraqi Journal for Electrical and Electronic Engineering*, vol. 17, no. 2, pp. 38-45, 2021. Available: 10.37917/ijeee.17.2.5 [Accessed 23 February 2022].

[5] S. Abdulwahab, H. Khleaf and M. Jassim, "EEG Motor-Imagery BCI System Based on Maximum Overlap Discrete Wavelet Transform (MODWT) and Machine learning algorithm", *Iraqi*

Journal for Electrical and Electronic Engineering, vol. 17, no. 2, pp. 38-45, 2021. Available: 10.37917/ijeee.17.2.5 [Accessed 23 February 2022].

[6] Akrout, A. Echtioui, R. Khemakhem and M. Ghorbel, "Artificial and Convolutional Neural Network of EEG-Based Motor imagery classification: A Comparative Study", *2020 20th International Conference on Sciences and Techniques of Automatic Control and Computer Engineering (STA)*, 2020. Available: 10.1109/sta50679.2020.9329317 [Accessed 23 February 2022].

[7] H. Amin, W. Mumtaz, A. Subhani, M. Saad and A. Malik, "Classification of EEG Signals Based on Pattern Recognition Approach", *Frontiers in Computational Neuroscience*, vol. 11, 2017. Available: 10.3389/fncom.2017.00103 [Accessed 23 February 2022].

[8] H. Amin, W. Mumtaz, A. Subhani, M. Saad and A. Malik, "Classification of EEG Signals Based on Pattern Recognition Approach", *Frontiers in Computational Neuroscience*, vol. 11, 2017. Available: 10.3389/fncom.2017.00103 [Accessed 23 February 2022].

[9] N. Md Isa, A. Amir, M. Ilyas and M. Razalli, "Motor imagery classification in Brain computer interface (BCI) based on EEG signal by using machine learning technique", *Bulletin of Electrical Engineering and Informatics*, vol. 8, no. 1, pp. 269-275, 2019. Available: 10.11591/eei.v8i1.1402 [Accessed 23 February 2022].

[10] E. Nurse, P. Karoly, D. Grayden and D. Freestone, "A Generalizable Brain-Computer Interface (BCI) Using Machine Learning for Feature Discovery", *PLOS ONE*, vol. 10, no. 6, p. e0131328, 2015. Available: 10.1371/journal.pone.0131328 [Accessed 23 February 2022].

[11] E. Nurse, P. Karoly, D. Grayden and D. Freestone, "A Generalizable Brain-Computer Interface (BCI) Using Machine Learning for Feature Discovery", *PLOS ONE*, vol. 10, no. 6, p. e0131328, 2015. Available: 10.1371/journal.pone.0131328 [Accessed 23 February 2022].

[12] N. Tibrewal, N. Leeuwis and M. Alimardani, "The Promise of Deep Learning for BCIs: Classification of Motor Imagery EEG using Convolutional Neural Network", *biorxiv.org*, 2021. [Online]. Available:

https://www.biorxiv.org/content/10.1101/2021.06.18.448960v1.full. [Accessed: 23- Feb- 2022].

[13] X. Zheng et al., "Task Transfer Learning for EEG Classification in Motor Imagery-Based BCI System", *Computational and Mathematical Methods in Medicine*, vol. 2020, pp. 1-11, 2020. Available: 10.1155/2020/6056383 [Accessed 23 February 2022]

COMPARING QUESTIONNAIRE RESULTS AND LEARNING OUTCOMES IN CLINICAL LABORATORY TRAINING PROGRAMS TO SUPPORT LEARNING IN JAPAN

K. Goto

Faculty of Medical Technology, Teikyo University, 173-8605, Itabashi, Tokyo, Japan.

Corresponding Author's Email: gotok@med.teikyo-u.ac.jp

Article History: Received May 19, 2022; Revised June 20, 2022; Accepted July 13, 2022

ABSTRACT: In Japan, the Ministry of Education, Culture, Sports, Science, and Technology requires every university to complete a learning behavior survey, assess the results, and disclose this information as part of the university's evaluation. This study examines the correlation between the results of the analysis conducted in a university for medical technologists and their learning outcomes, including GPA, graduation exam scores, and national exam scores. The learning behavior survey conducted in March 2020 included 345 participants studying medical technology. In total, 20 items were categorized based on seven factors. The results for the senior students were collated with their GPA scores, graduation exam scores, and national examination scores through factor analysis and multiple regression analysis using their scores and the factor scores. The results revealed that as students advance to upper grades, their efforts toward studying, such as study time, increase; however, no simple correlation exists between the increased study time and the resulting achievement. The medical technologist national exam scores were found to have a strong, positive correlation to three factors: effective use of leisure time, living environment, and observance of deadlines. The learning behavior survey analysis offers suggestions for students on the actions they must take to pass the national medical technologist exam.

KEYWORDS: *Universities; Students; Factor analysis; Surveys and Questionnaires; Regression analysis.*

1.0 INTRODUCTION

Higher education institutions in Japan include four-year universities and two-year and three-year junior colleges. Four-year universities award bachelor's degrees to university seniors, while junior colleges award associate's degrees and primarily provide vocational training. Students must graduate from a four-year university or a three-year junior college to take the national medical technologist examination. The enrollment rates for four-year universities and junior colleges were 45.1% and 54.8% in 2003 and 2017, respectively. While these rates have hardly changed since 2017, the number of four-year universities has increased from 669 in 2001 to 780 in 2017 [1].

In light of this, considering how to improve and maintain the quality of higher education is an urgent issue in university management. Since 2004, the government has required four-year universities, junior colleges, and technology colleges to be evaluated every seven years by an agency certified by the Ministry of Education, Culture, Sports, Science, and Technology. The ministry also requires that each university perform a learning behavior survey (using student questionnaires), tabulate the results, and make the results available to the public to aid high school students in choosing a university to attend.

In Japan, a national qualification is necessary to become a medical technologist. Medical technologists work at hospitals in Japan and conduct laboratory tests, such as blood tests, pathological tests, biochemical tests, microbiological tests, and tests for blood type at the time of blood transfusion. In addition, they conduct physiological function tests, such as electrocardiography, electroencephalography, and respiratory function tests. To take the national exam, candidates must graduate from a professional four-year university or a three-year college program. Currently, Japan has nearly 120 professional universities or colleges in total, and nearly 5,000 students take this national exam every year [2]. In 2020, the pass rate for the exam was 71.5%, with most universities working to increase the rate. Understanding the relationship between the national examination scores and the results of the learning behavior survey can help universities and colleges determine how best to increase the pass rate.

This study aimed to determine how students should be supported to pass the national examination of medical technologists. This was undertaken through a comparison of questionnaire results of

university students in all grades, factor analysis of the questionnaire results of fourth-year students (seniors), and multiple regression analysis of the factors and learning outcomes, including the GPA and the graduation exam scores, and the national exam scores.

2.0 METHODOLOGY

2.1 Questionnaire Target and Rating Items

The learning behavior survey using questionnaires was conducted in March 2020 (before COVID-19) at a university in Tokyo on 345 students studying medical technology: 99 first-year students (freshmen), 85 second-year students (sophomores), 90 third-year students (juniors), and 71 senior students. The results for the senior students were collated with their GPA, graduation, and national examination scores. Twenty rating items in total were utilized, and the evaluation criteria for each question are shown in Table 1.

Table 1: Results of the questionnaire graded on a 5-point Likert-type scale (mean±SD)

Item		Mean ± SD			
		Freshmen N=99	Sophomores N=85	Juniors N=90	Seniors N=71
Q1: 1: ≧8 hours, 2: ≧6 hours, 3: ≧4 hours, 4: ≧2 hours, 5: <2 hours	1: ≧8 hours, 2: ≧6 hours, 3: ≧4 hours, 4: ≧2 hours, 5: <2 hours	4.51 ± .05 a b	4.59 ± .07 a b	3.84 ± .10 c d	3.75 ± .12 c d
Q2: 1: Everyday, 2: Sometimes, 3: Only before the exam period, 4:Not study	1: Everyday, 2: Sometimes, 3: Only before the exam period, 4: Not	2.30 ± .07 a d	2.68 ± .10 b c	2.51 ± .08 c	2.26 ± .12 d
Q3: 1: Everyday, 2: Sometimes, 3: Hardly, 4: Not	1: Everyday, 2: Sometimes, 3: Hardly, 4: Not	3.70 ± .06 a b d	3.53 ± .07 a b c	1.90 ± .08 b c d	1.32 ± .07 a c d
Q4: 1: ≧5 days/week, 2: 4 days/week, 3: 3 days/week, 4: 2 days/week, 5: 1 day/week, 6: Not	1: ≧5 days/week, 2: 4 days/week, 3: 3 days/week, 4: 2 days/week, 5: 1 day/week, 6: Not	5.83 ± .04 a b	5.71 ± .08 a b	1.90 ± .08 c d	1.32 ± .07 c d
Q5: 1: Everyday, 2: Sometimes, 3: Hardly, 4: Not	1: Everyday, 2: Sometimes, 3: Hardly, 4: Not	2.45 ± .09 b	2.59 ± .11 a	2.30 ± .09 b d	2.80 ± .13 a c
Q6: 1: Greatly	1: Greatly increased, 2:	1.75 ± .05	1.85 ± .05	1.82 ± .06	1.59 ± .07

increased, 2: Increased, 3: Not changed, 4: Decreased, 5: Greatly decreased	Increased, 3: Not changed, 4: Decreased, 5: Greatly decreased	b	b	b	a c d
Q7: 1: Greatly increased, 2: Increased, 3: Not changed, 4: Decreased, 5: Greatly decreased	1: Greatly increased, 2: Increased, 3: Not changed, 4: Decreased, 5: Greatly decreased	2.18 ± .05 a b	2.06 ± .05 a b	1.76 ± .05 b c d	1.48 ± .06 a c d
Q8: 1: Greatly increased, 2: Increased, 3: Not changed, 4: Decreased, 5: Greatly decreased	1: Greatly increased, 2: Increased, 3: Not changed, 4: Decreased, 5: Greatly decreased	1.74 ± .05	1.87 ± .05 a b	1.67 ± .05 d	1.58 ± .07 d
Q9: 1: ≧5 days/week, 2: 4 days/week, 3: 3 days/week, 4: 2 days/week, 5: 1 day/week, 6: Not	1: ≧5 days/week, 2: 4 days/week, 3: 3 days/week, 4: 2 days/week, 5: 1 day/week, 6: Not	4.01 ± .15 a b	3.99 ± .15 a b	4.94 ± .11 c d	5.15 ± .13 c d
Q10: 1: ≧5 days/week, 2: 4 days/week, 3: 3 days/week, 4: 2 days/week, 5: 1 day/week, 6: Not	1: ≧5 days/week, 2: 4 days/week, 3: 3 days/week, 4: 2 days/week, 5: 1 day/week, 6: Not	5.30 ± .08 b d	4.88 ± .13 a b c	5.50 ± .11 d	5.75 ± .11 c d
Q11: 1: ≧5 days/week, 2: 4 days/week, 3: 3 days/week, 4: 2 days/week, 5: 1 day/week, 6: Not	1: ≧5 days/week, 2: 4 days/week, 3: 3 days/week, 4: 2 days/week, 5: 1 day/week, 6: Not	5.93 ± .03 d	5.59 ± .08 a c	5.82 ± .06 d	5.82 ± .09
Q12: 1: Everyday, 2: Sometimes, 3: Hardly, 4: Not	1: Everyday, 2: Sometimes, 3: Hardly, 4: Not	3.76 ± .05 a b	3.72 ± .07 a b	3.28 ± .09 c d	3.17 ± .11 c d
Q13: 1: ≧5 days/week, 2: 4 days/week, 3: 3 days/week, 4: 2 days/week, 5: 1 day/week, 6: Not	1: ≧5 days/week, 2: 4 days/week, 3: 3 days/week, 4: 2 days/week, 5: 1 day/week, 6: Not	5.92 ± .03 a d	5.46 ± .09 a c	5.74 ± .08 c d	5.70 ± .13
Q14: 1: Everyday, 2: Sometimes, 3: Hardly, 4: Not	1: Everyday, 2: Sometimes, 3: Hardly, 4: Not	3.66 ± .06 b	3.67 ± .06 b	3.62 ± .06 b	3.37 ± .09 a c d
Q15: 1: Live with parents, 2: Live alone, 3: Live at	1: Live with parents, 2: Live alone, 3: Live at dormitory, 4: Other	1.28 ± .05	1.21 ± .05 b	1.17 ± .05 b	1.38 ± .07 a d

dormitory, 4: Other					
Q16: 1: <30 min, 2: <60 min. 3: <90 min. 4: <120 min. 5: >120 min.	1: <30 min, 2: <60 min. 3: <90 min. 4: <120 min. 5: >120 min.	2.68 ± .12 b	2.68 ± .13 b	2.75 ± .11 b	2.26 ± .13 a c d
Q17: 1: Yes, 2: No	1: Yes, 2: No	1.28 ± .05 b	1.26 ± .05 b	1.24 ± .05 b	1.46 ± .06 a, b, c
Q18: 1: Yes, 2: No	1: Yes, 2: No	1.32 ± .05	1.36 ± .05	1.31 ± .05	1.37 ± .06
Q19: 1: Yes, 2: No	1: Yes, 2: No	1.02 ± .01	1.05 ± .02	1.01 ± .01 b	1.08 ± .03 a
Q20: 1: Submitted within the deadline, 2: Could not submit within the deadline, 3: No documents submitted	1: Submitted within the deadline, 2: Could not submit within the deadline, 3: No documents submitted	1.29 ± .07 b	1.42 ± .08 a b	1.19 ± .06 d	1.08 ± .04 c d

By referring to Table 1, data marked with "a" show a significant difference ($P<0.05$) in comparison with the data of "A junior"; data marked with "b" indicate a significant difference ($P<0.05$) in comparison with the data of "A senior"; data marked with "c" demonstrate a significant difference ($P<0.05$) in comparison with data of "A freshmen"; and data marked with "d" show a significant difference ($P<0.05$) in comparison with the data of "A sophomore."

2.2 Analysis

First, the questionnaire survey results were compared for each grade. Second, the factor analysis of the survey results for all the seniors was performed. Third, using the factor scores calculated from the 20 questions as independent variables, a multiple regression analysis was performed with the GPA score, graduation test results, or national exam score as the dependent variable. The relationship between the questionnaire and academic results was statistically examined. The factor analysis was performed on the learning behavior survey conducted in March 2020.

2.3 Statistical Analysis

IBM SPSS Statistics Version 22 was used for data storage, tabulation, and statistics generation. The data were also analyzed by factor and

regression analysis. The principal factor and varimax rotation methods were used to analyze the results for all 20 questionnaire survey items (listed in Table 2).

Table 2: Standardized regression weights of items on first-order factors and squared multiple correlations of predictors (principal factor method with varimax rotation)

	Factors*							h^{2*}
	F1	F2	F3	F4	F5	F6	F7	
Q1	0.82							0.75
Q2	0.74							0.63
Q3	0.62							0.46
Q4	0.54							0.55
Q5	0.37							0.29
Q6		0.90						0.84
Q7		0.83						0.77
Q8		0.76						0.60
Q9			0.77					0.70
Q10			0.62					0.48
Q11			0.61					0.67
Q12				0.72				0.53
Q13				0.63				0.55
Q14				0.50				0.45
Q15					0.83			0.75
Q16					-0.81			0.74
Q17						0.73		0.60
Q18						0.53		0.37
Q19						0.53		0.39
Q20							0.71	0.53

Note: F1: Quantity of self-study; F2: Awareness that it has been achieved; F3: Effective use of time other than study related to medical technology; F4: Collection of information; F5: Living environment; F6: Use of social media; F7: Observance of the deadline;
*h^2=communality

3.0 RESULTS

3.1 Questionnaire Survey

Table 1 presents the average value of the answers to each question. The senior students' results were significantly higher for most items than those in other grades. In other words, the higher the grade, the more enthusiastic the effort to study.

3.2 Factor Analysis of the Survey Results of Senior Students

A factor analysis was conducted on the questionnaire survey results to understand what factors affect student life. The Kaiser-Meyer-Olkin value of the scale for this analysis was 0.567, and Bartlett's test ($p < 0.00$) of sphericity was significant.

The factor analysis results are shown in Table 2. There were seven factors with a value over 1.00. One item, Q5, was excluded because its factor loading was less than 0.4. The seven factors, based on the theoretical structure, were as follows: Factor 1, the quantity of self-study (Q1 – Q4); Factor 2, awareness that it has been achieved (Q6 – Q8); Factor 3, effective use of leisure time (Q9 – Q11); Factor 4, collection of information (Q12 – Q14); Factor 5, the living environment (Q15 and Q16); Factor 6, use of social media (Q17 – Q19); and Factor 7, observance of deadlines.

3.3 Multiple Linear Regression Analysis

As shown in Table 3, Factor scores of 3, 5, and 7 had a significant ($p = 0.03$) association with the national examination score. The shorter the time spent on part-time work, club activities, and the lecture viewing system, the higher the national examination score tended to be ($p = 0.03$). However, the GPA and graduation exam scores were not related to these factors ($p > 0.05$; data not shown).

4.0 DISCUSSION

In this study, the results of the learning behavior survey completed by university medical technology students were collated with learning outcomes, such as GPA, graduation exam, and national examination

scores. The questionnaires consisted of 20 questions related to students' learning behavior. According to the results, the seniors spent the most time studying and felt that their knowledge had increased compared with the other students. Previous reports suggested that Japanese university students' average time studying at home for university lectures was 4.8, 5.4, 5.0, and 2.9 hours per week for freshmen, sophomores, juniors, and seniors, respectively [3].

Table 3: Results of the multiple regression analysis with the national examination score as the dependent variable

		Non-standardization coefficient			Standardization coefficient
		B	Standard error	p-value	β
F1	Quantity of self-study	1.53	1.54	0.32	0.13
F2	Awareness that it has been achieved	-1.73	1.48	0.25	0.15
F3	Effective use of leisure time	-3.51	1.52	0.03*	-0.29
F4	Collection of information	-1.54	1.68	0.36	-0.12
F5	Living environment	-3.55	1.58	0.03*	-0.28
F6	Use of social media	-1.11	1.70	0.52	-0.08
F7	Observance of deadline	4.15	1.90	0.03*	0.270

Note: *A significant effect on the national exam score

However, research shows that senior students spend more time studying on average [3]. Since they prioritize studying for the medical technologist national exam over research activities, study time tends to be longer as students' grade levels increase. Study time for freshman and sophomores varies greatly depending on the program of study. For example, 41% of freshmen and sophomore students in medical, dentistry, and pharmacy programs study for less than 5 hours/week, while 53.9% of freshmen and sophomore students in health-related fields such as nursing, medical technology, radiology, and nutrition, study for less than 5 hours/week. However, in Japan, the study time of students in social science and humanities programs tends to be the shortest: in these programs, over 80% and 66.3% of freshmen and sophomore students, respectively, study for less than 5 hours/week.

Further, students in health-related programs also tend to spend more time on graduation research than those in the social sciences and the humanities.

Using the questionnaire results of the senior students, factor analysis on the questions and correlation analysis using the factors and the academic performance, including GPA, graduation exam scores, and national examination scores, were performed to determine how to improve the learning effects at universities. It was confirmed that three of the seven extracted factors—effective use of leisure time, living environment, and compliance with promises (Factor 7)—were associated with national exam scores. Still, GPA scores and graduation exam scores were not associated with any factors. In particular, the length of study time did not directly affect the grades (Factor 1). Based on these results, how students use time effectively affects whether they pass the national exam, which affects the university's overall score.

5.0 CONCLUSION

The results in this study suggest that as students progress through the grades, they expend more effort on studying, such as increasing study time. Still, there was no simple correlation between increased study time and the final results. The national exam score for medical technologists was strongly correlated with three factors: effective use of leisure time, living environment of students, and observance of deadlines. The survey analysis results are expected to improve the passing rate of the national exam for medical technologists.

6.0 REFERENCES

[1] K. Goto, "Prediction of senior year medical students who do not pass the graduation exam by logistic analysis using data on gender, experience of repetition, and results of previous exams," *Medical Technologies Journal*, vol. 4, no. 1, pp. 497-503, 2020. doi:10.26415/2572-004X-vol4iss1p497-503

[2] K. Goto, "Measuring academic achievement based on selected exam subjects: The exam scores of medical technologist students," *Medical Technologies Journal*, vol. 3, no. 4, pp. 455-470, 2019. doi:10.26415/2572-004X-vol3iss4p455-470

[3] Y. Hamanaka, "Research on the educational and learning

environment that supports student growth," Reports of National Institute for Educational Policy Research, pp. 293-327, Tokyo [in Japanese].
https://www.nier.go.jp/05_kenkyu_seika/pdf_digest_h29/rep0301-all.pdf

REVIEW OF THE COMPLICATIONS IN PROSTHESIS MAKING & SERVICING

W.T. Chan

Faculty of Engineering and Technology, Multimedia University, 75450, Bukit Beruang, Melaka, Malaysia.

Corresponding Author's Email: wtchan@mmu.edu.my

Article History: Received May 25, 2022; Revised July 12, 2022; Accepted July 14, 2022

ABSTRACT: Prostheses are intended to restore the human body's appearance and return some functions lost due to the loss of limbs. The prosthesis industry exists for this purpose, as well as the servicing of the prostheses. However, there are complications in the design and installation of prostheses, as well as servicing them. Prosthesis usage is subjected to the specific circumstances of the recipient and is dependent on medical coverage for long-term servicing. The relatively low number of cases involving prostheses compared to other medical cases and the circumstantial differences between these cases prevent in-depth and comprehensive studies of the industry, preventing the establishment of standardized best practices. Despite this, research and development of improvements for recipients' problems continue, utilizing the latest technologies to address technical complications. This article consolidates the present-day complications of prosthesis making and servicing.

KEYWORDS: *Prosthesis, Prosthesis design, Affordability, Service complications.*

1.0 INTRODUCTION

The people who need prostheses may not always have the means to afford them. This is especially the case for those whose livelihood depends on their mobility. However, a prosthesis that can restore function in addition to their cosmetic purposes, i.e., masking the absence of limbs, tends to be costly [1]. On the other hand, the relationship between affordability and functionality is not rigidly proportional and is subjected to other factors such as material choices

and fulfillment of the intended purpose [2].

Although prostheses can provide aesthetics and function, they are devices that have to be delivered to the recipients in the first place. They also require maintenance and modification for the comfort of the recipients. Incidentally, some issues affect prostheses' quality, availability, and servicing [3].

In terms of scope, this article is primarily about prostheses for limbs. Cosmetic prostheses, e.g., cosmesis, and prostheses that reconstitute cognitive function, e.g., neuroprosthetics, and orthopedic and implant prostheses are not the focus. However, they occasionally mention overlapping factors such as using materials.

2.0 REVIEW OF HISTORICAL DEVELOPMENT OF PROSTHESES

The earliest prostheses were developed to address a relatively simple but sensitive issue: the absence of a body part that defines the silhouette of a human. This absence can lead to a sense of loss, leading to psychological and social issues [4].

As such, most early prostheses were made to resemble human limbs, though they did not have the means to move like them. They were also made using whatever technology that was available at the time, such as metalworking. In terms of functionality, they were mainly intended for acts of gesticulation. There were attempts to create prostheses for more than just this, such as the case of Gottfried von Berlichingen, having commissioned a prosthesis that could hold a sword [5]. There is a lack of technical documentation on whether the prosthesis can perform in combat, e.g., striking a lethal blow or parrying an attack. Yet, this case also involved revisions to the design of the prosthesis to expand functionality [5].

Incidentally, this indicates prosthesis design trends towards more functionality instead of mere appearance. However, present-day clinical studies on the functionality of prostheses show that most prostheses could not completely replicate the function of lost limbs, though there remains room for improvement [4]. Moreover, any advancement in prosthesis designs is still dependent on customizing prostheses for individuals, i.e., on a case-by-case basis [3]. This, in turn, prevents standardized manufacturing. Still, there have been efforts to establish categories of prostheses, e.g., transfemoral and transtibial

ones, which are needed to reduce the development time of the prostheses.

At this time of writing, general searches on prostheses on directories such as Scopus would reveal that one of the current prosthesis-making trends is 3D printing. 3D printing is one solution that addresses the complication of the different recipients having variations, such as different shapes of the stumps that would interface with the prostheses and different strengths and endurance in the remainder of their limbs. Other trends include using advanced materials and artificial intelligence in prostheses with electronics. However, these trends are optimistic takes that depend on technological advancements. Realistically, any advancement would pose complications as they address previous ones.

The following sections describe the complications in the prosthetics industry, both direct and indirect, and the solutions that have been pursued to address them.

3.0 MATERIALS

This section is mainly about the materials used in prostheses and their selection and sourcing complications.

3.1 The Consequence of Material Choices

The need for functional prostheses to be able to withstand the rigors of motion limits the range of materials that are practical for prostheses. In particular, materials have to be light enough because the rest of the recipient's body would have to support the weight of the prosthesis [6].

There is also the fact that most materials, on their own, do not come close to emulating the bone, sinew, and muscles of human limbs. Designs that make use of composite materials and/or multiple parts with different materials are attempts at such emulation. Still, the variety of materials can pose complications, such as how they react with each other and the location of the body they are installed onto [7].

Choosing materials means deliberation and testing of the materials, which in turn add to the development time and complications of the prostheses. Efforts to address this issue are usually pragmatic, such as

making decisions based on the availability of materials; any further complexity is only considered if complications arise from the default choices. In the present-day, knowledge bases about these decisions have been implemented in decision-making and simulation software to reduce time spent on deliberation [8].

3.2 Sourcing of Materials

Research and development (R&D) efforts in materials include finding alternative sources of suitable materials. This is so that the use of materials for prosthesis-making does not compete with the same materials for other practical endeavors. Incidentally, shortage of materials has been cited to be a considerable problem in making prostheses, such as in resource-strapped nations like Tanzania [9].

Contemporary R&D, in this matter, attempts to derive viable materials from cheaper sources, such as fiber from plants [10]. Such advancements do diversify the sources of materials for prostheses; in some cases, short-term tests of their strength suggest that they can perform just as well as prostheses that are wholly made of the usual materials such as fiberglass [11]. However, these also pose the complication of manufacturing methods involving more types of materials, thus increasing the complexity of developing prostheses.

The long-term viability of alternate materials is unclear due to the lack of in-depth studies on the durability of these materials. On the other hand, certain alternative materials may provide certain advantages. For example, biodegradable materials are utilized in prosthetic implants, albeit with risks of toxicity from the decomposition [12]. These may be helpful in the disposal of limb prostheses that are not intended for long-term use, such as those for growing children.

A particular avenue of the solution to sourcing materials is using recycled waste, especially plastic waste. Incidentally, this is being pursued in countries with pervasive issues of plastic waste, such as the Philippines [13]. However, as this is a nascent solution, the long-term complications of using recycled materials have yet to be made clear. For example, residual chemicals remain in recycled plastics [14], which can pose a health risk; there has yet to be an in-depth study on this.

3.3 The Durability of Materials & Associated Complications of Maintenance and Replacement

Most prostheses for adults are intended for long-term use. They have to endure the weight of their users and withstand the rigors of providing function. Thus, the selection of materials has to consider the durability of the materials and how this would affect the frequency of maintenance and replacement.

However, due to the differences in the lifestyles of recipients, there have not been many comprehensive experiments and studies comparing the effect of the usage of different materials on the frequency of maintenance and replacement. Indeed, in this matter and practice, complex factors like availability of materials, comfortable fitting for the recipient, and safety of the recipient take precedence over cost comparisons of materials [2][15].

4.0 DESIGN

This section concerns the complications posed by implementing the technical designs for prostheses.

4.1 Designs of Prostheses & Associated Complications of Maintenance

The design, the installation method, and the expected stresses on the prostheses while they are being used contribute greatly to the rate of wear on the prostheses and thus their needs for repairs and replacement. However, as with the aforementioned matter of choices of materials, there are not many comprehensive studies on the costs associated with prosthesis designs due to the variety of recipients and their circumstances. Attempts at these studies greatly depend on the contribution of data from prosthetic clinics and the workshops that provide service to the former, as well as the consent of the patients [16]. Furthermore, due to the relatively low number of cases involving prosthesis use compared to cases in other fields of medicine and rehabilitation, any source of data that is substantial enough to account for a diversity of factors would be subjected to the issue of significant time spans, i.e., some cases may be so many years apart from each other that the techniques that are used may not be fairly comparable [16].

4.2 Fabrication of Materials for Prostheses

Although the designs of prostheses in their entirety are not comparable due to the many factors involved, there are still efforts to compare options with each other on a lower level. One of these is fabricating the materials that would be shaped into a prosthesis.

Incidentally, R&D efforts in this matter address the notion of substituting one material for another with the idea of having different materials compensating for each other [7]. Furthermore, there can be additional potentially beneficial effects from having mixtures of materials. For example, fabricating composite materials for implants instead of homogeneous materials promotes bone growth [17].

3D printing, otherwise known as additive manufacturing, has been implemented in the manufacture of prosthetics, especially for customized designs and where manufacturing by molding is not convenient [18]. 3D printing is feasible for custom designs of parts away from the connection between the prosthesis and the recipient's body. However, the connection, i.e., the fitting of the prosthesis, requires frequent monitoring and modification to suit the patient's comfort. Computer-aided design (CAD) and finite element analysis (FEA), which goes hand-in-hand with 3D printing, do not reliably accelerate this process [19].

4.3 Inclusion of Advanced Technology

Electrical and electronic components have been implemented in the designs of prostheses to improve response and expand mobility, though the improvements have not been universal for every recipient [20]. R&D for such prostheses continues, including additional types of sensors and associated programming, more sophisticated osseointegration, and utilization of augmented and virtual reality in rehabilitation [21].

However, including such advanced technologies and techniques also increases the costs of prostheses. For example, an arm prosthesis with electromyography (EMG) control for the fingers of its hand can cost up to US$50,000, which is very high compared to a powered prosthesis that only grips and has few other complex motions and which purportedly has material costs of just AU$ 30 [22]. As of now, there have not been any comprehensive studies that yield a clear and consistent relationship between the efficacy of prosthetics and their

level of technology.

R&D efforts to implement advanced technology while minimizing costs continue through the means described in sections III. On the other hand, the inclusion of any technology to improve and expand function is expected to increase the complexity of the design, thus introducing additional costs through other avenues like fitting calibration and acclimation efforts [21].

Furthermore, due to the case-by-case nature of prosthetic designs, the correlation between improved function and advanced technology is not certain; the study carried out by Carey et al. shows that the circumstances of recipients and their satisfaction are varied such that there is no conclusive correlation between the two [23].

5.0 DISTRIBUTION

This section concerns the complications in delivering prostheses to recipients and servicing them afterward.

5.1 General Availability of Services and Associated Complications

Prostheses are devices that require installation and maintenance. Consequently, any consideration of complications should consider long-term contributors as well as the hurdles of getting the prostheses to the recipient.

Incidentally, there is not much data on prostheses in low-income countries, which is due to the low number of practitioners of prosthetics in these places as well as the consequently low number of reports on prosthetic use [24]. This scarcity is due to underlying causes such as poor quality of life and lack of a comprehensive healthcare system for reasons such as the prevalence of violent conflict [24].

Thus, the diminished capacity for healthcare services would also affect the distribution of prosthesis usage. There has to be a significant investment to establish a healthcare system that can support the use of prosthetics [25].

5.2 Regional Issues

After fabricating prostheses, they and the recipient must be brought together for fitting and testing. Prosthesis clinics allow this process to

be performed safely and reliably, but these clinics are not common. In particular, recipients in developing countries must travel considerable distances and inconvenient terrain to reach the clinics [26]. The solution to this problem of remoteness would seem to be the establishment of more clinics while making prostheses more affordable (as has been described in previous sections), usually through the efforts of non-governmental organizations (NGOs) [26].

However, even if the investment costs can be addressed, other obstacles prevent the proliferation of clinics and distribution of prostheses, such as cultural complications regarding understanding the need for prostheses [27]. The causes for these obstacles can be socio-politically sensitive. For example, there is contention over the issue of prostheses for former Turkish soldiers who are amputees. Their veteran status entitles them to have prostheses, but they have to make payments and risk repossession upon failure to make payments [28].

As has been mentioned in the previous section, the solution has to include the establishment of a healthcare system that can support the use of prostheses. Furthermore, the system must be standardized nationwide instead of relegated to local authorities like in Canada [29]. This is to have uniform service quality and prevent traveling to have satisfactory service elsewhere.

6.0 RECIPIENT'S NEEDS

Prostheses must be made to fit the recipient while also providing function, so there will be complications in satisfying the recipient.

6.1 Disparity in Service

The extent of medical coverage for recipients of prostheses is not universal. The cause of the recipient's need for a prosthesis can be a factor in the difference in the quality of service between recipients. For example, in the USA, military veteran amputees have access to more options and complete coverage of costs. In contrast, civilians have to obtain coverage through their insurance schemes, the benefits of which can vary significantly. Ethical issues among the practitioners of prosthetics can arise from such disparity [30].

A significant aspect of prosthesis service is refitting; as a recipient acclimates to the prosthesis, the recipient may require readjustment of

the fitting. This incurs costs of testing and fabrication of new prosthesis parts. Due to disparities in servicing, the recipient may have limited refits, which can affect satisfaction and rejection of the prosthesis [31].

6.2 Ease of Use and Comfort

Most prostheses, including state-of-the-art ones, are not within the complete control of the recipient like an actual healthy limb would be. Thus, ease of use is important in their acceptance of the prostheses. Yet, this factor is also determined by their lifestyle and culture. For example, Cambodian recipients still observe religious rites, such as kneeling to pray. These activities are complicated by prostheses that are not designed to facilitate any activity other than walking or standing, e.g., lower limb prostheses chafe with the back of the thighs when kneeling [32].

The general solution is to include considerations of comfort in the design of the prostheses. However, this increases the complexity of the designs and necessitates more tests, though using FEA can reduce the need to make more prototypes [33].

Since prostheses involve skin contact with the prosthesis's materials, there is the issue of comfort or loss thereof from this contact. The design of the prostheses has to include consideration of and testing for dermal allergies that the patient may have [15].

The matter of ease of use and comfort also reinforces the notion that prosthesis designs must be done on a case-by-case basis. This, in turn, recalls the aforementioned issue of the recipients needing the necessary medical coverage that allows for modifications of the prostheses.

7.0 CONCLUSION

The advancement of technology has contributed to the design of prostheses that perform better in restoring performance. However, implementing state-of-the-art technologies like robotics and neuro-cybernetics to improve response times and modern manufacturing techniques like 3D printing has also increased the complexity of prostheses. This poses significant long-term concerns such as ease of maintenance and availability of expertise to service the prostheses.

Efforts to solve this problem include the exploration of alternative sources

of materials, e.g., molding using recycled plastics. Furthermore, Knowledge on prosthesis designs accumulated, documented, and disseminated over many years has been implemented in software designed to support and accelerate prosthesis development. This angle of addressing the issue of prosthesis complications can be contributed to via further sharing of ideas and case studies, as well as utilization of the latest physics simulations to predict the performance of prosthesis designs.

However, solutions that rely on R&D could only address problems of technical nature in the field of prostheses. There are problems with more complicated causes, such as cultural issues and healthcare systems that could not completely support or protect recipients of prostheses. There are also the subjective matters of the recipient's eagerness to have a prosthesis and satisfaction of having one, which leads to the provision of prostheses being a case-by-case matter and thus posing a difficulty in having comprehensive studies on the use of prostheses.

Lastly, reviews on matters in the field of prostheses and analytical studies of prostheses would indubitably be hampered by a lack of cases [34]. The need for prosthetics is not expected to diminish entirely due to circumstances that prevent medical treatment required to save limbs from amputation. However, the scarcity of data would continue to worsen due to medical advancements in limb salvage and limb-sparing that are focused on preventing amputation and, in turn preventing the use of prostheses.

On the other hand, advancements in the field of prostheses can be applied in the field of reconstructive surgery and rehabilitation, e.g., prosthetic implants. Thus, in the event of diminishing prospects for the field of prostheses due to a reduction of patients needing them, practitioners and researchers of prosthetics can pivot their efforts to the latter, such as in the case of the development of materials for osseointegration [35].

8.0 REFERENCES

[1] V. H. Nagaraja, J. H. M. Bergmann, D. Sen & M. S. Thompson, "Examining the needs of affordable upper limbprosthetic users in India: Aquestionnaire-based survey," Technology and Disability, vol. 1, pp. 1-10, 2016.

[2] A. N. Amsan, A. K. Nasution & M. H. Ramlee, "A Short Review on the Cost, Design, Materials and Challenges of the Prosthetics Leg Development and Usage," Advances in Engineering Research, vol. 190, pp. 59 to 64, 2019.

[3] M.C. Jochan & K. Ravikumar, "A Review on Prosthetics and Orthotics for Amputees and Disabled," Journal of Critical Reviews, vol. 7, issue 15, pp. 2175-2189, 2020.

[4] K. J. Zuo & J. L. Olson, "The evolution of functional hand replacement: From iron prostheses to hand transplantation," Plastic Surgery, vol. 22, issue 1, pp. 44 – 51, 2014.

[5] K. Ashmore, S. Cialdella, A. Giuffrida, E. Kon, M. Marcacci & B. D/ Matteo, "ArtiFacts: Gottfried "Götz" von Berlichingen—The "Iron Hand" of the Renaissance," Clinical Orthopaedics and Related Research, vol. 477, issue 9, pp. 2002-2004, 2019.

[6] G. A. Ramadhani, S. Susmartini, L. Herdiman & I. Priadythama, "Advanced composite-based material selection for prosthetic socket application in developing countries," Cogent Engineering, vol. 7, issue 1, 2020.

[7] H. Mehboob & S.H. Chang, "Application of composites to orthopedic prostheses for effective bone healing: A review," Composite Structures, vol. 118, pp. 328-341, 2014.

[8] T. Mangera, F. Kienhöfer, K.J. Carlson, M. Conning, A. Brown & G. Govender, "Optimal material selection for the construction of a paediatric prosthetic knee," Proceedings of the Institution of Mechanical Engineers, Part L: Journal of Materials: Design and Applications, vol. 232, issue 2, pp. 1-12, 2018.

[9] J.M. Ibrahim, S. Serrano, A.M. Caldwell, E.N. Eliezer, B.T. Haonga & D.W. Shearer, "Barriers to Prosthetic Devices at a Tanzanian Hospital," East African Orthopaedic Journal, vol. 13, pp. 40-47, 2019.

[10] A. Campbell, S. Sexton, C.J. Schaschke, H. Kinsman, B. McLaughlin & M. Boyle "Prosthetic limb sockets from plant-based composite materials," Prosthetics and Orthotics International, vol. 36, issue 2, pp. 181-189, 2012.

[11] E. Gashawtena, B. Sirahbizu & A. Kidane, "Review on Alternate Materials for Producing Low Cost Lower Limb Prosthetic Socket," Journal of Material Sciences & Engineering, vol. 10, issue 6, pp. 1-6, 2021.

[12] M. Prakasam, J. Locs, K. Salma-Ancane, D. Loca, A. Largeteau & L. Berzina-Cimdina, "Biodegradable Materials and Metallic Implants—A Review," Journal of Functional Biomaterials, vol. 8, issue 4, pp. 1-15, 2017.

[13] F.N.R. Arcilla, A.K.M. Garcia, M.A.R. Sarthou, A.M.A. Lugue, A/ D. M. Rubiano, "Recycled plastics: An alternative material for prosthetic

check socket fabrication," UERM Health Sciences Journal, vol. 8, issue. 2, pp. 115-121, 2019.

[14] J. N. Hahladakis, C.A. Velis, R. Weber, E. Iacovidou & P. Purnell, "An overview of chemical additives present in plastics: Migration, release, fate and environmental impact during their use, disposal and recycling," Journal of Hazardous Materials, vol. 344, pp. 179-199, 2018.

[15] C. Quintero-Quiroz & V.Z. Pérez, "Materials for lower limb prosthetic and orthotic interfaces and sockets: Evolution and associated skin problems," Revista de la Facultad de Medicina, vol. 67, issue 1, pp. 117, 2019.

[16] E.E. Haggstrom, E. Hansson & K. Hagberg, "Comparison of prosthetic costs and service between osseointegrated and conventional suspended transfemoral prostheses," Prosthetics and Orthotics International, vol. 37, issue 2, pp. 152-160, 2012.

[17] R.C. Petersen, "Bisphenyl-Polymer/Carbon-Fiber-Reinforced Composite Compared to Titanium Alloy Bone Implant," International Journal of Polymer Science, Polymeric Biomaterials for Tissue Engineering Applications, 2011.

[18] A. Manero, P. Smith, J. Sparkman, M. Dombrowski, D. Courbin, A. Kester, I. Womack & A. Chi, "Implementation of 3D Printing Technology in the Field of Prosthetics: Past, Present, and Future," International Journal of Environmental Research and Public Health, vol. 16, issue 9, pp. 1-15, 2019.

[19] Y. Wang, Q. Tan, F. Pu, D. Boone & M. Zhang, "A Review of the Application of Additive Manufacturing in Prosthetic and Orthotic Clinics from a Biomechanical Perspective," Engineering, vol. 6, issue 11, pp. 1258-1266, 2020.

[20] A. Chadwell, L. Kenney, S. Thies, A. Galpin and J. Head, "The Reality of Myoelectric Prostheses: Understanding What Makes These Devices Difficult for Some Users to Control," Frontiers in Neurorobotics, vol. 10, issue 7, pp. 1-21, 2016.

[21] T.J. Bates, J.R. Fergason & S.N. Pierrie, "Technological Advances in Prosthesis Design and Rehabilitation Following Upper Extremity Limb Loss," Current Reviews in Musculoskeletal Medicine, vol. 13, issue 4, pp. 485-493, 2020.

[22] N. Sreenivasan, D.F.U. Gutierrez, P. Bifulco, M. Cesarelli, U. Gunawardana, & G.D. Gargiulo, "Towards Ultra Low-Cost Myoactivated Prostheses," BioMed Research International, vol. 2018, Article ID 9634184, pp. 1-14, 2018.

[23] S. L. Carey, D..J. Lura & M.J. Highsmith, "Differences in myoelectric and body-powered upper-limb prostheses: Systematic literature

review," The Journal of Rehabilitation Research and Development, vol. 52, issue 3, pp. 247-262, 2015.

[24] C.S. Harkins, A. McGarry & A. Buis, "Provision of prosthetic and orthotic services in low-income countries: A review of the literature," Prosthetics and Orthotics International, vol. 37, issue 5, pp. 353-361. 2013.

[25] S. Shahabi, S. Pardhan, A.A. Teymourlouy, D. Skempes, S. Shahali, P. Mojgani, M. Jalali & K.B. Lankarani, "Prioritizing solutions to incorporate Prosthetics and Orthotics services into Iranian health benefits package: Using an analytic hierarchy process," PLOS ONE, 2021.

[26] M. Greenberg, K. Mehta & S. Ritter, "Access to prosthetic devices in developing countries: Pathways and challenges," IEEE 2015 Global Humanitarian Technology Conference, pp. 45-50, 2015.

[27] D. Wyss, S. Lindsay, W.L. Cleghorn & J. Andrysek, "Priorities in lower limb prosthetic service delivery based on an international survey of prosthetists in low- and high-income countries," Prosthetics and Orthotics International, vol. 39, issue 2, pp. 102-111, 2015.

[28] S.C. Açıksöz, "Prosthetic Debts: Economies of War Disability in Neoliberal Turkey," Current Anthropology, vol. 61, issue 21, pp. 76-86, 2020.

[29] C. Howard, D.K. Saraswat, G. McLeod, A. Young, D. Jeong & J. Lam, "Canada's Prosthetic Coverage: A Review of Provincial Prostheic Policy," Canadian Prosthetics & Orthotics Journal, vol. 2, issue 2, pp. 1-9, 2019.

[30] P.F. Pasquina, A.J. Carvalho & T.P. Sheehan, "Ethics in Rehabilitation: Access to Prosthetics and Quality Care Following Amputation," American Medical Association Journal of Ethics, vol. 17, issue 6, pp. 535-546, 2015.

[31] E. Biddiss, P. McKeever, S. Lindsay & T. Chau, "Implications of prosthesis funding structures on the use of prostheses: experiences of individuals with upper limb absence," Prosthetics and Orthotics International, vol. 35, issue 2, pp. 215-224, 2011.

[32] N. Ramstrand, A. Maddock, M. Johansson & L. Felixon, "The lived experience of people who require prostheses or orthoses inthe Kingdom of Cambodia: A qualitative study," Disability and Health Journal, vol. 14, pp. 1-8, 2021.

[33] M.H. Baharuddin, A.M.A. Rashid, A.K. Nasution, H.S. Gan & M.H. Ramlee, "Patient-Specific Design of Passive Prosthetic Leg for Transtibial Amputee: Analysis Between Two Different Designs,"

Malaysian Journal of Medicine and Health Sciences, vol. 17, issue 4, pp. 228-234, 2021.

[34] B.J. Hafner & A.B. Sawers, "Issues affecting the level of prosthetics research evidence: Secondary analysis of a systematic review," Prosthetics and Orthotics International, vol. 40, issue 1, pp. 31 to 43, 2016.

[35] V. Karthik, S.K. Pabi & S.K.R. Chowdhury, "Development of hydroxyapatite/polyvinyl alcohol bionanocomposite for prosthesis implants," IOP Conference Series: Materials Science and Engineering, vol. 314, pp. 1-7, 2018.

Appendix

Revised Article

COMPARING QUESTIONNAIRE RESULTS AND LEARNING OUTCOMES IN CLINICAL LABORATORY TRAINING PROGRAMS TO SUPPORT LEARNING IN JAPAN

K. Goto[1,*]

[1]Faculty of Medical Technology, Teikyo University, Tokyo, 173-8605, Japan

[*]Corresponding Author's Email: gotok@med.teikyo-u.ac.jp

Article History: Received May 19, 2022; Revised Oct 18, 2022;

ABSTRACT: In Japan, the Ministry of Education, Culture, Sports, Science, and Technology requires every university to complete a learning behavior survey, assess the results, and disclose this information as part of the university's evaluation. This study examines the correlation between the results of the analysis conducted in a university for medical technologists and their learning outcomes, including GPA, graduation exam scores, and national exam scores. The learning behavior survey conducted in March 2020 included 345 participants studying medical technology. In total, 20 items were categorized based on seven factors. The results for the senior students were collated with their GPA scores, graduation exam scores, and national examination scores through factor analysis and multiple regression analysis using their scores and the factor scores. The results revealed that as students advance to upper grades, their efforts toward studying, such as study time, increase; however, no simple correlation exists between the increased study time and the resulting achievement. The medical technologist national exam scores were found to have a strong, positive correlation to three factors: effective use of leisure time, living environment, and observance of deadlines. The learning behavior survey analysis offers suggestions for students on the actions they must take to pass the national medical technologist exam.

KEYWORDS: *Universities; Students; Factor analysis; Surveys and Questionnaires; Regression analysis.*

1.0 INTRODUCTION

Higher education institutions in Japan include four-year universities and two-year and three-year junior colleges. Four-year universities

award bachelor's degrees to university seniors, while junior colleges award associate's degrees and primarily provide vocational training. Students must graduate from a four-year university or a three-year junior college to take the national medical technologist examination. The enrollment rates for four-year universities and junior colleges were 45.1% and 54.8% in 2003 and 2017, respectively. While these rates have hardly changed since 2017, the number of four-year universities has increased from 669 in 2001 to 780 in 2017 [1].

In light of this, considering how to improve and maintain the quality of higher education is an urgent issue in university management. Since 2004, the government has required four-year universities, junior colleges, and technology colleges to be evaluated every seven years by an agency certified by the Ministry of Education, Culture, Sports, Science, and Technology. The ministry also requires that each university perform a learning behavior survey (using student questionnaires), tabulate the results, and make the results available to the public to aid high school students in choosing a university to attend.

In Japan, a national qualification is necessary to become a medical technologist. Medical technologists work at hospitals in Japan and conduct laboratory tests, such as blood tests, pathological tests, biochemical tests, microbiological tests, and tests for blood type at the time of blood transfusion. In addition, they conduct physiological function tests, such as electrocardiography, electroencephalography, and respiratory function tests. To take the national exam, candidates must graduate from a professional four-year university or a three-year college program. Currently, Japan has nearly 120 professional universities or colleges in total, and nearly 5,000 students take this national exam every year [2]. In 2020, the pass rate for the exam was 71.5%, with most universities working to increase the rate. Understanding the relationship between the national examination scores and the results of the learning behavior survey can help universities and colleges determine how best to increase the pass rate.

This study aimed to determine how students should be supported to pass the national examination of medical technologists. This was undertaken through a comparison of questionnaire results of university students in all grades, factor analysis of the questionnaire results of fourth-year students (seniors), and multiple regression analysis of the factors and learning outcomes, including the GPA and the graduation exam scores, and the national exam scores.

2.0 METHODOLOGY

2.1 Questionnaire Target and Rating Items

The learning behavior survey using questionnaires was conducted in March 2020 (before COVID-19) at a university in Tokyo on 345 students studying medical technology: 99 first-year students (freshmen), 85 second-year students (sophomores), 90 third-year students (juniors), and 71 senior students. The results for the senior students were collated with their GPA, graduation, and national examination scores. Twenty rating items in total were utilized, and the evaluation criteria for each question are shown in Table 1.

Table 1: Results of the questionnaire graded on a 5-point Likert-type scale (mean±SD)

Item		Mean ± SD			
		Freshmen N=99	Sophomores N=85	Juniors N=90	Seniors N=71
Q1: How much time did you spend daily studying for a university lecture at home on average?	1: ≧8 hours, 2: ≧6 hours, 3: ≧4 hours, 4: ≧2 hours, 5: <2 hours	4.51 ± .05 a b	4.59 ± .07 a b	3.84 ± .10 c d	3.75 ± .12 c d
Q2: How often did you study at home for university lectures?	1: Everyday, 2: Sometimes, 3: Only before the exam period, 4: Not	2.30 ± .07 a d	2.68 ± .10 b c	2.51 ± .08 c	2.26 ± .12 d
Q3: How often did you study for the national exam at home?	1: Everyday, 2: Sometimes, 3: Hardly, 4: Not	3.70 ± .06 a b d	3.53 ± .07 a b c	1.90 ± .08 b c d	1.32 ± .07 a c d
Q4: How many days a week did you use the university library?	1: ≧5 days/week, 2: 4 days/week, 3: 3 days/week, 4: 2 days/week, 5: 1 day/week, 6: Not	5.83 ± .04 a b	5.71 ± .08 a b	1.90 ± .08 c d	1.32 ± .07 c d
Q5: How often did you study for experiment and practical training at home?	1: Everyday, 2: Sometimes, 3: Hardly, 4: Not	2.45 ± .09 b	2.59 ± .11 a	2.30 ± .09 b d	2.80 ± .13 a c
Q6: How much did your knowledge of liberal arts and specialties increase?	1: Greatly increased, 2: Increased, 3: Not changed, 4: Decreased, 5: Greatly decreased	1.75 ± .05 b	1.85 ± .05 b	1.82 ± .06 b	1.59 ± .07 a c d

Q7: How much did your knowledge of the national exam increase?	1: Greatly increased, 2: Increased, 3: Not changed, 4: Decreased, 5: Greatly decreased	2.18 ± .05 a b	2.06 ± .05 a b	1.76 ± .05 b c d	1.48 ± .06 a c d
Q8: How much did your specialty skills increase?	1: Greatly increased, 2: Increased, 3: Not changed, 4: Decreased, 5: Greatly decreased	1.74 ± .05	1.87 ± .05 a b	1.67 ± .05 d	1.58 ± .07 d
Q9: How often did you work part-time on average per week?	1: ≧5 days/week, 2: 4 days/week, 3: 3 days/week, 4: 2 days/week, 5: 1 day/week, 6: Not	4.01 ± .15 a b	3.99 ± .15 a b	4.94 ± .11 c d	5.15 ± .13 c d
Q10: What was the average weekly frequency of club activities?	1: ≧5 days/week, 2: 4 days/week, 3: 3 days/week, 4: 2 days/week, 5: 1 day/week, 6: Not	5.30 ± .08 b d	4.88 ± .13 a b c	5.50 ± .11 d	5.75 ± .11 c d
Q11: How many times did you watch past lectures on average per week using the class recording system?	1: ≧5 days/week, 2: 4 days/week, 3: 3 days/week, 4: 2 days/week, 5: 1 day/week, 6: Not	5.93 ± .03 d	5.59 ± .08 a c	5.82 ± .06 d	5.82 ± .09
Q12: How long did you use the office hours for consultation on study and daily life with teachers?	1: Everyday, 2: Sometimes, 3: Hardly, 4: Not	3.76 ± .05 a b	3.72 ± .07 a b	3.28 ± .09 c d	3.17 ± .11 c d
Q13: How often did you use the computer room for self-study on average per week?	1: ≧5 days/week, 2: 4 days/week, 3: 3 days/week, 4: 2 days/week, 5: 1 day/week, 6: Not	5.92 ± .03 a d	5.46 ± .09 a c	5.74 ± .08 c d	5.70 ± .13
Q14: How often did you consult with the clerical staff?	1: Everyday, 2: Sometimes, 3: Hardly, 4: Not	3.66 ± .06 b	3.67 ± .06 b	3.62 ± .06 b	3.37 ± .09 a c d
Q15: Please tell us your resident situation.	1: Live with parents, 2: Live alone, 3: Live at dormitory, 4: Other	1.28 ± .05	1.21 ± .05 b	1.17 ± .05 b	1.38 ± .07 a d
Q16: How long was the transit time?	1: <30 min, 2: <60 min. 3: <90 min. 4: <120 min. 5: >120 min.	2.68 ± .12 b	2.68 ± .13 b	2.75 ± .11 b	2.26 ± .13 a c d
Q17: Do you use SNS (Instagram)?	1: Yes, 2: No	1.28 ± .05 b	1.26 ± .05 b	1.24 ± .05 b	1.46 ± .06 a, b, c
Q18: Do you use SNS (Twitter)?	1: Yes, 2: No	1.32 ± .05	1.36 ± .05	1.31 ± .05	1.37 ± .06
Q19: Do you use SNS (Line)?	1: Yes, 2: No	1.02 ± .01	1.05 ± .02	1.01 ± .01 b	1.08 ± .03 a

Q20: Did you submit the required documents within the deadline?	1: Submitted within the deadline, 2: Could not submit within the deadline, 3: No documents submitted	1.29 ± .07 b	1.42 ± .08 a b	1.19 ± .06 d	1.08 ± .04 c d

By referring to Table 1, data marked with "a" show a significant difference (P<0.05) in comparison with the data of "A junior"; data marked with "b" indicate a significant difference (P<0.05) in comparison with the data of "A senior"; data marked with "c" demonstrate a significant difference (P<0.05) in comparison with data of "A freshmen"; and data marked with "d" show a significant difference (P<0.05) in comparison with the data of "A sophomore."

2.2 Analysis

First, the questionnaire survey results were compared for each grade. Second, the factor analysis of the survey results for all the seniors was performed. Third, using the factor scores calculated from the 20 questions as independent variables, a multiple regression analysis was performed with the GPA score, graduation test results, or national exam score as the dependent variable. The relationship between the questionnaire and academic results was statistically examined. The factor analysis was performed on the learning behavior survey conducted in March 2020.

2.3 Statistical Analysis

IBM SPSS Statistics Version 22 was used for data storage, tabulation, and statistics generation. The data were also analyzed by factor and regression analysis. The principal factor and varimax rotation methods were used to analyze the results for all 20 questionnaire survey items (listed in Table 1).

Table 2. Standardized regression weights of items on first-order factors and squared multiple correlations of predictors (principal factor method with varimax rotation)

	Factors*							h^{2*}
	F1	F2	F3	F4	F5	F6	F7	
Q1	0.82							0.75
Q2	0.74							0.63
Q3	0.62							0.46
Q4	0.54							0.55
Q5	0.37							0.29
Q6		0.90						0.84
Q7		0.83						0.77
Q8		0.76						0.60
Q9			0.77					0.70
Q10			0.62					0.48
Q11			0.61					0.67
Q12				0.72				0.53
Q13				0.63				0.55
Q14				0.50				0.45
Q15					0.83			0.75
Q16					-0.81			0.74
Q17						0.73		0.60
Q18						0.53		0.37
Q19						0.53		0.39
Q20							0.71	0.53

Note: F1: Quantity of self-study; F2: Awareness that it has been achieved; F3: Effective use of time other than study related to medical technology; F4: Collection of information; F5: Living environment; F6: Use of social media; F7: Observance of the deadline;
*h^2=communality

3.0 RESULTS

3.1 Questionnaire Survey

Table 1 presents the average value of the answers to each question. The senior students' results were significantly higher for most items than

those in other grades. In other words, the higher the grade, the more enthusiastic the effort to study.

3.2 Factor Analysis of the Survey Results of Senior Students

A factor analysis was conducted on the questionnaire survey results to understand what factors affect student life. The Kaiser-Meyer-Olkin value of the scale for this analysis was 0.567, and Bartlett's test ($p < 0.00$) of sphericity was significant.

The factor analysis results are shown in Table 2. There were seven factors with a value over 1.00. One item, Q5, was excluded because its factor loading was less than 0.4. The seven factors, based on the theoretical structure, were as follows: Factor 1, the quantity of self-study (Q1 – Q4); Factor 2, awareness that it has been achieved (Q6 – Q8); Factor 3, effective use of leisure time (Q9 – Q11); Factor 4, collection of information (Q12 – Q14); Factor 5, the living environment (Q15 and Q16); Factor 6, use of social media (Q17 – Q19); and Factor 7, observance of deadlines.

3.3 Multiple Linear Regression Analysis

As shown in Table 3, Factor scores of 3, 5, and 7 had a significant ($p = 0.03$) association with the national examination score. The shorter the time spent on part-time work, club activities, and the lecture viewing system, the higher the national examination score tended to be ($p = 0.03$). However, the GPA and graduation exam scores were not related to these factors ($p > 0.05$; data not shown).

4.0 DISCUSSION

In this study, the results of the learning behavior survey completed by university medical technology students were collated with learning outcomes, such as GPA, graduation exam, and national examination scores. The questionnaires consisted of 20 questions related to students' learning behavior. According to the results, the seniors spent the most time studying and felt that their knowledge had increased compared with the other students. Previous reports suggested that Japanese university students' average time studying at home for university lectures was 4.8, 5.4, 5.0, and 2.9 hours per week for freshmen,

sophomores, juniors, and seniors, respectively [3].

Table 3. Results of the multiple regression analysis with the national examination score as the dependent variable

		Non-standardization coefficient			Standardization coefficient
		B	Standard error	p-value	β
F1	Quantity of self-study	1.53	1.54	0.32	0.13
F2	Awareness that it has been achieved	-1.73	1.48	0.25	0.15
F3	Effective use of leisure time	-3.51	1.52	0.03*	-0.29
F4	Collection of information	-1.54	1.68	0.36	-0.12
F5	Living environment	-3.55	1.58	0.03*	-0.28
F6	Use of social media	-1.11	1.70	0.52	-0.08
F7	Observance of deadline	4.15	1.90	0.03*	0.270

Note: *A significant effect on the national exam score

However, research shows that senior students spend more time studying on average [3]. Since they prioritize studying for the medical technologist national exam over research activities, study time tends to be longer as students' grade levels increase. Study time for freshman and sophomores varies greatly depending on the program of study. For example, 41% of freshmen and sophomore students in medical, dentistry, and pharmacy programs study for less than 5 hours/week, while 53.9% of freshmen and sophomore students in health-related fields such as nursing, medical technology, radiology, and nutrition, study for less than 5 hours/week. However, in Japan, the study time of students in social science and humanities programs tends to be the shortest: in these programs, over 80% and 66.3% of freshmen and sophomore students, respectively, study for less than 5 hours/week. Further, students in health-related programs also tend to spend more time on graduation research than those in the social sciences and the humanities.

Using the questionnaire results of the senior students, factor analysis on the questions and correlation analysis using the factors and the academic performance, including GPA, graduation exam scores, and national examination scores, were performed to determine how to

improve the learning effects at universities. It was confirmed that three of the seven extracted factors—effective use of leisure time, living environment, and compliance with promises (Factor 7)—were associated with national exam scores. Still, GPA scores and graduation exam scores were not associated with any factors. In particular, the length of study time did not directly affect the grades (Factor 1). Based on these results, how students use time effectively affects whether they pass the national exam, which affects the university's overall score.

5.0 CONCLUSION

The results in this study suggest that as students progress through the grades, they expend more effort on studying, such as increasing study time. Still, there was no simple correlation between increased study time and the final results. The national exam score for medical technologists was strongly correlated with three factors: effective use of leisure time, living environment of students, and observance of deadlines. The survey analysis results are expected to improve the passing rate of the national exam for medical technologists.

6.0 REFERENCES

[1] K. Goto, "Prediction of senior year medical students who do not pass the graduation exam by logistic analysis using data on gender, experience of repetition, and results of previous exams," *Medical Technologies Journal*, vol. 4, no. 1, pp. 497-503, 2020. doi:10.26415/2572-004X-vol4iss1p497-503

[2] K. Goto, "Measuring academic achievement based on selected exam subjects: The exam scores of medical technologist students," *Medical Technologies Journal*, vol. 3, no. 4, pp. 455-470, 2019. doi:10.26415/2572-004X-vol3iss4p455-470

[3] Y. Hamanaka, "Research on the educational and learning environment that supports student growth," Reports of National Institute for Educational Policy Research, pp. 293-327, Tokyo [in Japanese]. https://www.nier.go.jp/05_kenkyu_seika/pdf_digest_h29/rep0301-all.pdf

Penumbra™

62

68

72

RED™

REPERFUSION CATHETERS

REDglide™ Technology
Designed to enhance delivery in tortuosity

62
.062" ID
1.93mm (0.76") OD
138cm Length

68
.068" ID
2.13mm (0.84") OD
132cm Length

72
.072" ID
2.16mm (0.85") OD
132cm Length